

Macrocyclic Pyridyl Polyoxazoles: Selective RNA and DNA G-Quadruplex Ligands as Antitumor Agents

Suzanne G. Rzuczek,[†] Daniel S. Pilch,^{‡,§} Angela Liu,^{‡,§} Leroy Liu,^{‡,§} Edmond J. LaVoie,^{§,†} and Joseph E. Rice*,[†]

[†]Department of Medicinal Chemistry, Ernest Mario School of Pharmacy, Rutgers—The State University of New Jersey, 160 Frelinghuysen Road, Piscataway, New Jersey 08854-8020, [‡]Department of Pharmacology, The University of Medicine and Dentistry of New Jersey, Robert Wood Johnson Medical School, Piscataway, New Jersey 08854-5635, and [§]The Cancer Institute of New Jersey, New Brunswick, New Jersey 08901

Received January 15, 2010

The synthesis of a series of 24-membered pyridine-containing polyoxazole macrocycles is described. Seventeen new macrocycles were evaluated for cytotoxic activity against RPMI 8402, KB-3, and KB-3 cell lines that overexpress the efflux transporters MDR1 (KBV-1) and BCRP (KBH5.0). Macrocycles in which the pyridyl-polyoxazole moiety is linked by a 1,3-bis(aminomethyl)phenyl group with a 5-(2-aminoethyl)- (**18**) or a 5-(2-dimethylaminoethyl)- substituent (**19**) displayed the greatest cytotoxic potency. These compounds exhibit exquisite selectivity for stabilizing G-quadruplex DNA with no stabilization of duplex DNA or RNA. Compound **19** stabilizes quadruplex mRNA that encodes the cell-cycle checkpoint protein kinase Aurora A to a greater extent than the quadruplex DNA of a human telomeric sequence. These data may suggest a role for G-quadruplex ligands interacting with mRNA being associated with the biological activity of macrocyclic polyoxazoles. Compound **19** has significant *in vivo* anticancer activity against a human breast cancer xenograft (MDA-MB-435) in athymic nude mice.

Introduction

Compounds that selectively stabilize the G-quadruplex conformation of nucleic acids represent a unique and novel class of anticancer agents.¹ The discovery of the natural product telomestatin, which stabilizes G-quadruplex DNA and inhibits telomerase, prompted research aimed at the design of similar G-quadruplex interactive agents.² Telomestatin (Figure 1), a 24-membered macrocycle composed of seven oxazole rings and one thiazoline, has a unique molecular architecture that permits efficient π -stacking interactions of its unsaturated heterocyclic rings with p-orbitals on the guanines of a nucleic acid when they are arranged as a planar G-quartet within a quadruplex.³ Studies have suggested that one telomestatin molecule stacks at each terminal G-quartet within a quadruplex to give a 2:1 complex. Moreover, telomestatin stabilizes G-quadruplex DNA in a selective manner, with minimal interaction with duplex DNA.⁴ A large number of polycyclic aromatic hydrocarbons and heterocycles have been designed and synthesized as G-quadruplex stabilizers but most are less selective than telomestatin.⁵ The design and development of compounds that interact with high selectivity with G-quadruplexes are critical to the elucidation of the pharmacological effects of such agents and for establishing the potential clinically utility of this class of anticancer agents.⁶

Recently, the synthesis of a series of 24-membered macrocycles incorporating six oxazole rings (two trisoxazole arrays) joined through an amino acid residue has been reported.⁷ The lead compound hexaoxazole-divaline (HDXD^a) has two valine residues connecting the tris-oxazole moieties and stabilizes G-quadruplex DNA to an extraordinary degree with no detectable stabilization of single stranded, duplex, or triplex DNA (Figure 1).^{7c} HDXD has moderate cytotoxicity toward tumors cells (average $IC_{50} \sim 0.5 \mu M$), which is comparable to that reported for telomestatin.⁸ HDXD induces robust apoptosis in both telomerase positive and telomerase negative cells within 16 h, causes M-phase cell cycle arrest, and reduces the expression of the M-phase checkpoint regulator Aurora A.⁹ These effects are not observed for the non-G-quadruplex stabilizing 24-membered macrocycle TXTLeu (tetraoxazole-tetraleucine, Figure 1). Formulation of HDXD for *in vivo* assessment of its antitumor activity proved difficult given its physicochemical properties. Efforts were focused on developing analogues that retain the exquisite selectivity for G-quadruplexes, exhibit enhanced anticancer activity in cell cultures, and possess improved physicochemical properties to permit facile formulation and *in vivo* administration. Toward this goal, HDXD analogues with water-solubilizing amino-alkyl groups having two to four-carbon chains replacing one or both isopropyl groups were synthesized and evaluated for their ability to selectively stabilize G-quadruplex DNA and for their cytotoxicity toward tumor cells.¹⁰ Each analogue that was prepared in these studies required a lengthy (>20 step) synthesis that is not readily amenable to the synthesis of quantities of compound that might be required for extensive *in vivo* evaluation against various human tumor xenografts. It was reasoned that a new structure scaffold was needed that

*To whom correspondence should be addressed. Phone: 732-445-5382. Fax: 732-445-6312. E-mail: jrice@rci.rutgers.edu.

^aAbbreviations: Boc, *tert*-butoxycarbonyl; Cbz, benzylloxycarbonyl; DAST, (diethylamino)sulfur trifluoride; DBU, 1,8-diazabicyclo[5.4.0]undec-7-ene; DMF, *N,N*-dimethylformamide; EDC, *N*-(3-dimethylaminopropyl)-*N'*-ethylcarbodiimide; HOBr, 1-hydroxybenzotriazole; HDXD, hexaoxazole divaline; TFA, trifluoroacetic acid; TFAA, trifluoroacetic anhydride; TIPS, triisopropylsilyl.

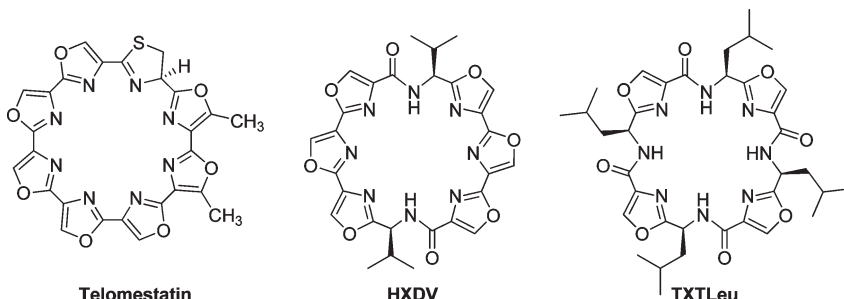
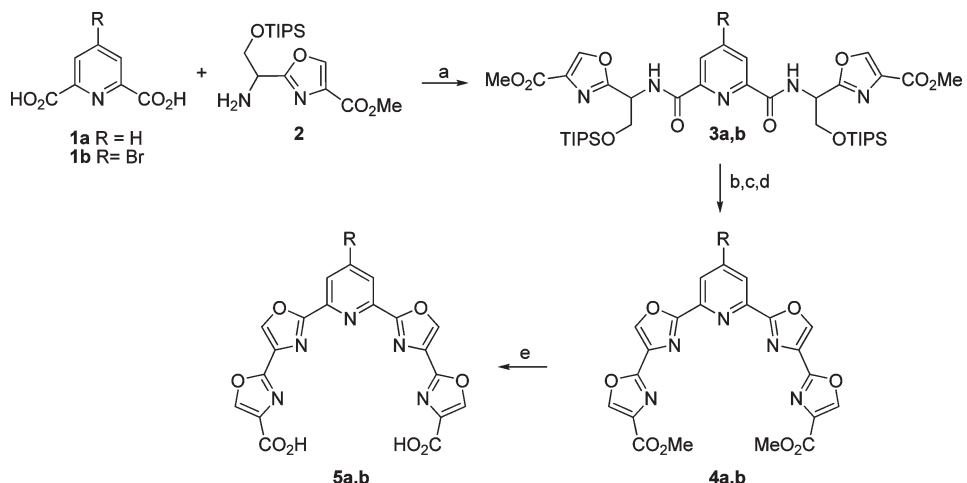


Figure 1. Structures of telomestatin, HXDV, and TXTLeu.

Scheme 1^a



^a Reagents and conditions: (a) EDC, HOBT, 2,6-lutidine, DMF, 0 °C to rt; (b) HF-pyridine, rt; (c) DAST, CH₂Cl₂, -78 °C; (d) BrCCl₃, DBU, CH₃CN, 0 °C to rt; (e) for R=H, LiOH, THF/H₂O, Δ; for R=Br, LiBr, DBU, THF/H₂O, Δ.

can be readily prepared on a multigram scale and easily modified to provide a variety of macrocyclic analogues for evaluating the effect of structure on selective G-quadruplex stabilization and antitumor activity. The design and synthesis of such a scaffold and its elaboration into a series of 24-membered macrocycles is the subject of this investigation. Cytotoxicity data is provided for each targeted macrocycle. On the basis of these data, compound **19** was selected and evaluated for in vivo efficacy against the human breast tumor xenograft MDA-MB-435. In addition, the potential of several of these compounds to selectively stabilize G-quadruplexes formed in DNA and RNA was determined.

Results and Discussion

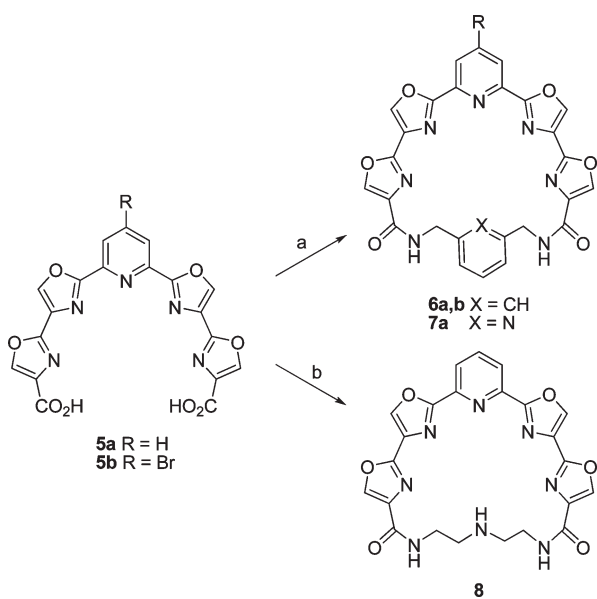
Previous results from our laboratories suggested that a somewhat planar or slightly puckered 24-membered macrocycle with a minimum of five heterocyclic rings is optimal for efficient G-quadruplex stabilization.⁷ A scaffold having a symmetrical array of five contiguous heterocyclic rings bearing identical functionality at each end was envisioned to which a variety of bifunctional linkers could be connected to complete the macrocycle. For ease of synthesis a pyridine having a bis(oxazole) moiety at the 2- and 6-positions appeared to be a logical choice. Readily available pyridine-2,6-dicarboxylic acid (**1a**) was condensed with oxazole **2**^{10a} to give bis(amide) **3a** in 80% yield (Scheme 1). The TIPS groups were removed with HF-pyridine complex, and the resulting diol was treated with DAST to effect cyclodehydration to the bis(oxazoline).¹¹ Dehydrogenation to tetraoxazole **4a** was accomplished with

BrCCl₃/DBU.¹² The esters were then hydrolyzed to afford scaffold **5a** in an overall yield of 64%. A second scaffold **5b** was designed to incorporate a 4-bromo substituent on the pyridine which was intended to provide a point of attachment for a variety of functionality at that position on the completed macrocycle. Compound **5b** was prepared in 47% overall yield from 4-bromopyridine-2,6-dicarboxylic acid¹³ (**1b**) by an analogous route as **5a**, except that hydrolysis of the ester groups was achieved by treatment with LiBr and DBU to avoid displacement of the bromine from the pyridine ring.¹⁴

The conversion of **5a,b** into 24-membered macrocycles required them to be condensed with a seven atom bifunctional linker. Among the linkers initially employed for this purpose were diethylenetriamine, 1,3-bis(aminomethyl)benzene, and 2,6-bis(aminomethyl)pyridine.¹⁵ A dilute solution (2 mM) of **5a** or **5b** in DMF was treated with EDC, HOBT, and 2,6-lutidine followed by the linker and stirred at room temperature for 2 d (Scheme 2). The yields of macrocycles **6a**, **6b**, and **7** were 30%, 35%, and 22% respectively. Macrolactamization using diethylenetriamine proved more challenging as extensive polymerization occurred using the standard procedure. Stirring **5a** for 3 h with copper(II) triflate prior to treatment with EDC, HOBT, and the diamine linker allowed for macro-lactamization to occur to give macrocycle **8** in 15% yield after 2 d. Presumably the copper acts as a template to hold the open ends of **5a** in a conformation more favorable for macrocyclization.

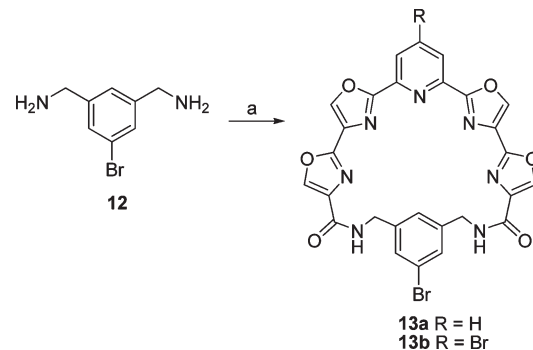
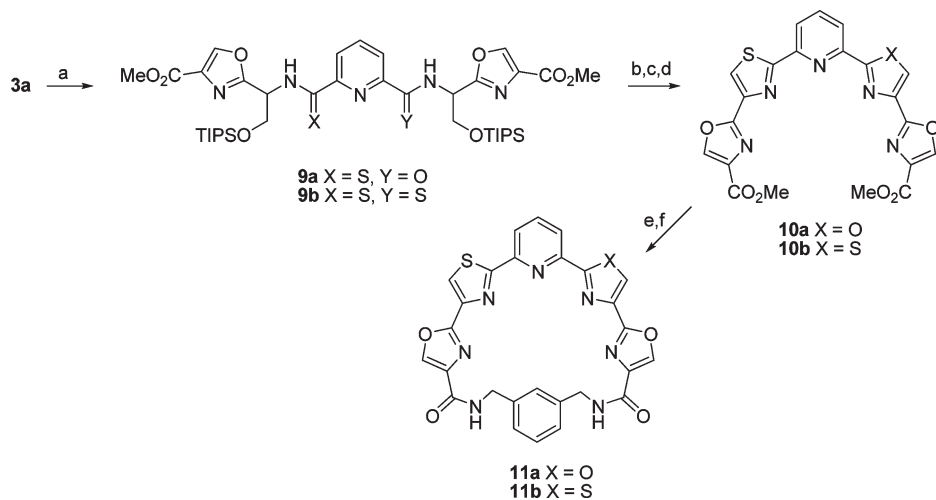
The replacement of one or two oxazole rings by thiazoles was also investigated (Scheme 3). To that end, treatment of **3a** with 1 equiv of Lawesson's reagent¹⁶ in toluene at 80 °C gave

monothioamide **9a** in good yield. In the presence of excess Lawesson's reagent, bis(thioamide) **9b** was formed. The conversion of **9a,b** into pyridyl tetraazole derivatives **10a,b** in overall yields of 56% and 79%, respectively was achieved using an identical sequence as employed for **4a,b**. The esters were hydrolyzed with LiOH and macrocyclization of **10a** with 1,3-bis(aminomethyl)benzene afforded **11a** in 33% yield. Surprisingly, similar treatment of **10b** failed to give any of the bis(thiazole) macrocycle **11b**. Performing the macrocyclization in a stepwise manner, however, provided a solution to this problem. Thus condensation of **10b** with the commercially available mono-Boc derivative of 1,3-bis(aminomethyl)benzene followed by treatment with TFA afford the mono-amide in 68% for the two steps. Macrocyclization using EDC then gave the desired macrocycle **11b** in 43% yield.

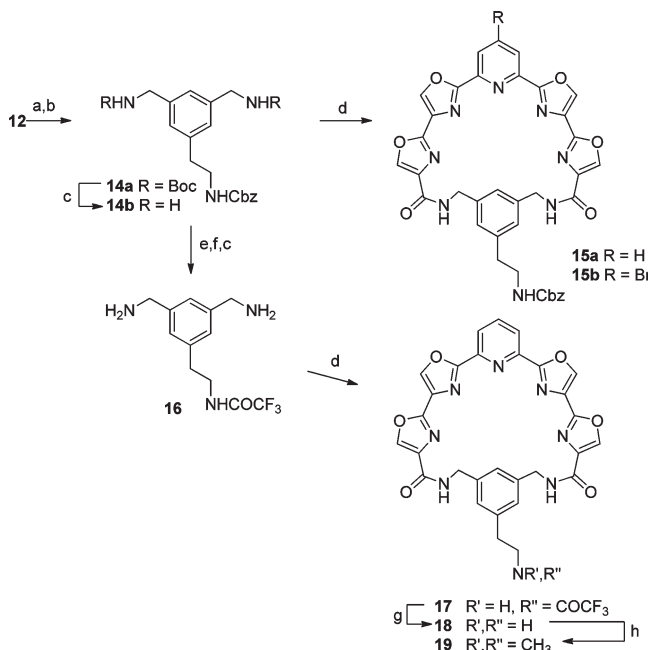
Scheme 2^a

The ability to prepare macrocycles having water-solubilizing groups attached to either the pyridine or phenyl ring was a critical element to allow for the test compounds to be readily formulated and administered in the assessment of their *in vivo* antitumor activity. It was envisioned that a suitably positioned halide on either the pyridine ring, as in **6b**, or on the phenyl ring could serve as a handle for the attachment of substituents via transition-metal catalyzed coupling reactions. To that end, 1,3-bis(aminomethyl)-5-bromobenzene **12** was prepared¹⁷ as an additional linker (Scheme 4). Macrocyclization of **12** with **5a** and **5b** afforded compounds **13a** and **13b** in 58 and 22% yield, respectively. Unfortunately, all attempts to derivatize **6b**, **13a**, or **13b** by Suzuki–Miyaura coupling with potassium [2-(benzyloxycarbonylamino)ethyl]trifluoroborate¹⁸ led primarily to the debromo compound **6a**. It is possible that the intact macrocycle chelates the palladium catalyst and prevents it from participating in the coupling reaction.

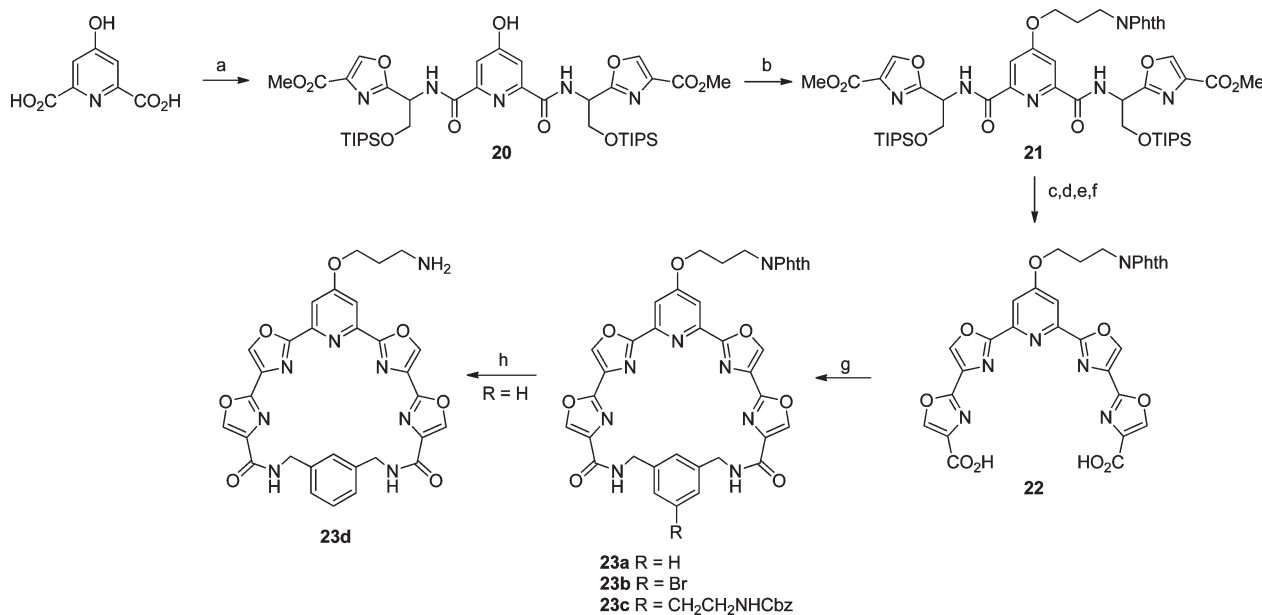
The water-solubilizing substituent could, however, be attached to the phenyl linker prior to macrocyclization. This required that the primary amino groups of **12** be protected as *tert*-butyl carbamate (Boc) derivatives (Scheme 5). Suzuki–Miyaura coupling of the resulting bromo compound with the same trifluoroborate reagent in the presence of PdCl₂(dppf)·CH₂Cl₂ and Cs₂CO₃ afforded the desired product

Scheme 4^aScheme 3^a

14a in 79% yield. Removal of the Boc groups with trifluoroacetic acid (TFA) and macrocyclization with **5a** and **5b** afforded compounds **15a** and **15b** in identical 42% yields. Removal of the Cbz group from **15a**, however, proved troublesome under a variety of hydrogenolysis conditions, affording the primary amine in very low yield. Therefore, **14a**

Scheme 5^a

^a Reagents and conditions: (a) Boc_2O , Et_3N , CH_2Cl_2 , rt; (b) $\text{CbzNH-CH}_2\text{CH}_2\text{BF}_3\text{K}$, $\text{PdCl}_2(\text{dpf})\cdot\text{CH}_2\text{Cl}_2$, Cs_2CO_3 , toluene/ H_2O , 80 °C; (c) TFA, CH_2Cl_2 , 0 °C; (d) **5a** or **5b** (2 mM in DMF), EDC, HOBT, 2,6-lutidine, rt, 2 d; (e) 1 atm H_2 , 20% $\text{Pd}(\text{OH})_2/\text{C}$, EtOH, rt; (f) TFAA, pyridine, CH_2Cl_2 , 0 °C; (g) K_2CO_3 , MeOH, Δ ; (h) HCHO (aq), $\text{NaBH}(\text{OAc})_3$, MeOH/ CH_2Cl_2 , rt.

Scheme 6^a

^a Reagents and conditions: (a) **2**, EDC, HOBT, 2,6-lutidine, DMF, 0 °C to rt; (b) $\text{Br}(\text{CH}_2)_3\text{NPhth}$, DBU, DMF, 60 °C; (c) HF-pyridine, rt; (d) DAST, CH_2Cl_2 , −78 °C; (e) BrCCl_3 , DBU, CH_2Cl_2 , 0 °C to rt; (f) LiCl, DMF, Δ ; (g) 1,3-bis(aminomethyl)benzene or **12** or **14**, (2 mM in DMF), EDC, HOBT, 2,6-lutidine, rt, 2 d; (h) $\text{H}_2\text{NNH}_2\cdot\text{H}_2\text{O}$, EtOH, Δ .

was subjected to hydrogenolysis over $\text{Pd}(\text{OH})_2/\text{C}$ to remove the Cbz group in quantitative yield. Protection of the amine as a trifluoroacetamide (TFAA, pyridine) was then followed by removal of the Boc groups (TFA) and gave diamine **16**. Macrocyclization of **16** with **5a** afforded compound **17** in 25% yield. The trifluoroacetamide was removed upon treatment with K_2CO_3 in MeOH to give **18**. A portion of **18** was reductively methylated using aqueous formaldehyde and sodium triacetoxyborohydride to give the *N,N*-dimethylamino derivative **19**.

The synthesis of a third scaffold having a basic side-chain attached to the pyridine ring (Scheme 6) proved necessary due to our inability to derivatize bromo compound **6b**. Chelidonic acid (4-hydroxypyridine-2,6-dicarboxylic acid) was coupled with oxazole **2** to form bis(amide) **20**. Treatment with *N*-(3-bromopropyl)phthalimide and DBU afforded pyridyl ether **21**. Removal of the TIPS protecting groups, cyclodehydration with DAST, and dehydrogenation with $\text{BrCCl}_3/\text{DBU}$ gave scaffold **22** after removal of the ester groups using LiCl in refluxing DMF. This was subjected to macrocyclization using 1,3-bis(aminomethyl)benzene, **12**, and **14a** (after removal of the Boc groups) to give macrolactams **23a–c**. Treatment of **23a** with hydrazine hydrate gave primary amine **23d**.

Each macrocycle was evaluated for cytotoxic activity against human lymphoblastoma RPMI 8402, human epidermoid carcinoma KB3-1, and KB3-1 cell lines that overexpress the efflux transporters MDR1 (KBV-1) and BCRP (KBH5.0) (Table 1). The parent macrocycle **6a**, with a 1,3-bis(aminomethyl)phenyl group linking the ends of scaffold **5a** displays modest cytotoxic potency against RPMI 8402 and KB3-1 ($\text{IC}_{50} \sim 1 \mu\text{M}$). Replacement of that linker with either 2,6-bis(aminomethyl)pyridyl, **7a**, or diethylenetriamine, **8**, results in a loss of activity. The replacement of one oxazole ring of **6a** with a thiazole (**11a**) resulted in a 4-fold increase in activity against KB3-1, but had no effect on RPMI 8402 cells. Substitution of a second oxazole by thiazole (**11b**), however, resulted in a complete loss of activity. The loss of activity for diethylenetriamine derivative

Table 1. Cytotoxicity of Macroyclic Pyridyl Polyoxazoles^a

compd	IC ₅₀ (μM)			
	RPMI 8402	KB3-1 wt	KBV-1 + MDR1	KBH5.0 + BCRP
HXDV	0.6	0.4	8.5	0.5
6a	1.05	1.2	4.5	1.5
6b	0.3	0.15	2.0	1.0
7a	> 5	> 5	> 5	> 5
8	> 10	4.0	> 10	> 10
11a	1.0	0.26	> 10	> 10
11b	> 10	> 10	> 10	> 10
13a	0.3	0.06	> 10	1.0
13b	> 10	> 10	> 10	> 10
15a	0.12	0.12	> 10	> 10
15b	1.0	0.6	> 10	> 10
17	0.17	0.07 ^b	> 10 ^b	> 10 ^b
18	0.09	0.03 ^b	> 10 ^b	0.14 ^b
19	0.18	0.04 ^b	> 10 ^b	0.55 ^b
23a	4.5	0.4	> 10	> 10
23b	1.0	1.0	> 10	> 10
23c	> 10	> 10	> 10	> 10
23d	5.0	3.0	> 10	> 10

^a Values represent the average of three experiments. ^b Values represent the average of four experiments.

8 might be related to its less rigid structure as compared to **6a**, although the effect of including a strongly basic secondary amine within the macrocycle cannot be discounted. A substantial difference in lipophilicity exists between thiazole ($\log P = 0.77$) and oxazole ($\log P = -0.59$), which may help to explain why substitution of a second oxazole by thiazole (compound **11b**), results in a loss of activity relative to monothiazole **11a**. At the present time, however, we can offer no explanation for the results obtained with dipyridyl derivative **7a**.

Attachment of a single bromine at either the 5-position of the benzene ring (**13a**) or the 4-position of the pyridine **6b** results in a 3-fold increase in cytotoxic potency against RPMI 8402 and about a 10-fold increase in activity against KB3-1 as compared to unsubstituted benzene derivative **6a**. Simultaneous substitution of bromine on both the benzene and pyridine rings (**13b**), however, results in a loss of all activity. This might again be an effect of the increased lipophilicity of **13b** as opposed to **6b** and **13a**. A similar, although not so dramatic, trend is observed for the 5-[2-(benzyloxycarbonylamino)ethyl]-1,3-bis(aminomethyl)-phenyl-linked macrocycles **15a** and **15b**. Compound **15a**, which is unsubstituted on the pyridine is 5–10 times more active than **15b**, which has a bromine on the 4-position of the pyridine ring. The Cbz-protected 2-aminoethyl derivative **15a** is approximately 1 order of magnitude more potent than parent compound **6a**. A change in the amine protecting group to trifluoroacetamide **17** has little effect on activity. Both primary amine **18** and tertiary amine **19** have potent activity (30–40 nM) against KB3-1 cells and slightly weaker activity (90–180 nM) against RPMI 8402 cells. It is also noteworthy that while **18** and **19** are both substrates for MDR1, as evidenced by their total lack of activity against KBV-1, they retain similar cytotoxicity against KBH5.0 relative to KB3-1, cells indicating that they are not substrates for the efflux transporter BCRP.

The effect of attachment of a large group ($\text{OCH}_2\text{CH}_2\text{CH}_2\text{NPhth}$) on the pyridine ring at its 4-position was to substantially lower activity. For example, comparison of 4-bromophenyl derivatives **23b** and **13a** reveals a 3–16 fold loss of activity for the substituted pyridyl derivative **23b** in RPMI 8402 and KB3-1 cells. Similarly, for compounds having a protected 2-aminoethyl substituent on the phenyl ring, activity drops from 120 nM for **15a** to > 10 μM with the attachment of the large substituent on the pyridine ring (**23c**).

Within this series, only **23a** with an unsubstituted phenyl ring exhibited moderate activity against KB3-1 cells (0.4 μM) but was largely inactive (IC_{50} 4.5 μM) against the RPMI 8402 cell line. Changing the nature of the terminal group on the (3-aminopropyl)oxy to primary amine **23d** did not enhance cytotoxic potency.

HXDV and four selected macrocyclic pyridyl polyoxazoles (**6a**, **11b**, **18**, and **19**) were evaluated for their ability to selectively bind and stabilize quadruplex versus duplex DNA and RNA in the presence of physiological concentrations of K^+ ions (150 mM). We used salmon testes (ST) DNA and poly(rA)·poly(rU) as representative models of duplex DNA and RNA, respectively. As a representative model of quadruplex DNA, we used the human telomeric sequence $d[\text{T}_2\text{G}_3(\text{T}_2\text{AG}_3)_3\text{A}]$, which we denote as hTel. Patel and co-workers have shown that the structure adopted by $d[\text{T}_2\text{G}_3(\text{T}_2\text{AG}_3)_3\text{A}]$ in K^+ solution is an intramolecular (3 + 1) G-quadruplex in which three strands are oriented in one direction and the fourth strand is oriented in the opposite direction.¹⁹ In an effort to explore ligand binding interactions with quadruplex RNA, we used a putative quadruplex-forming sequence ($r[\text{AG}_4\text{CG}_2\text{CUG}_2\text{UCG}_2\text{AGUG}_2\text{C}]$) derived from the 5'-untranslated region of the mRNA that encodes the cell-cycle checkpoint protein kinase Aurora A (AurA).

Figure 2 shows the UV melting profiles (depicted in their first derivative forms) of the four nucleic acids described above in the absence and presence of HXDV and **19**. The ligand-induced changes, if any, in the transition temperatures (T_{tran}) corresponding to the maxima or minima of these first-derivative melting profiles are listed in Table 2, as are the corresponding changes in T_{tran} values derived from melting profiles (not shown) conducted in the presence of **6a**, **11b**, and **18**. The presence of neither ligand alters the thermal stability of ST duplex DNA or poly(rA)·poly(rU) duplex RNA to any significant extent, with any observed changes in T_{tran} being within the experimental uncertainty. This observation is consistent with little or no duplex DNA or RNA binding on the part of any of the five macrocyclic polyoxazoles tested here. We previously observed a similar behavior for HXDV.^{7,10}

In marked contrast to their negligible impacts on the thermal stabilities of the DNA and RNA target duplexes, HXDV, **6a**, **18**, and **19** increase the T_{tran} value of the hTel DNA quadruplex by 11.5, 7.5, 21.0, and 20.5 °C, respectively. These results are not only indicative of binding to hTel but also provide information with regard to the relative affinities of the compounds for the host DNA quadruplex. In this connection, the relative extents to which ligands stabilize a target nucleic acid are typically correlated with the relative binding affinities of the ligands for the target.²⁰ Our hTel UV melting results are therefore consistent with the affinities of HXDV, **6a**, **18**, and **19** for the target DNA quadruplex following the hierarchy **18** ≈ **19** > HXDV > **6a**. It is perhaps not surprising that **18** and **19** exhibit a greater apparent affinity for the hTel quadruplex than HXDV or **6a**, because, unlike HXDV and **6a** (which are nonionic), **18** and **19** both contain basic amine functionalities that adopt positive charges at the physiologically relevant pH of 7.5 used in the UV melting studies. Note that, unlike HXDV, **6a**, **18**, and **19**, compound **11b** exerts no impact on the thermal stability of the hTel quadruplex. This observation coupled with the duplex results described above suggests that **11b** binds neither the duplex nor the quadruplex nucleic acid form. The lack of

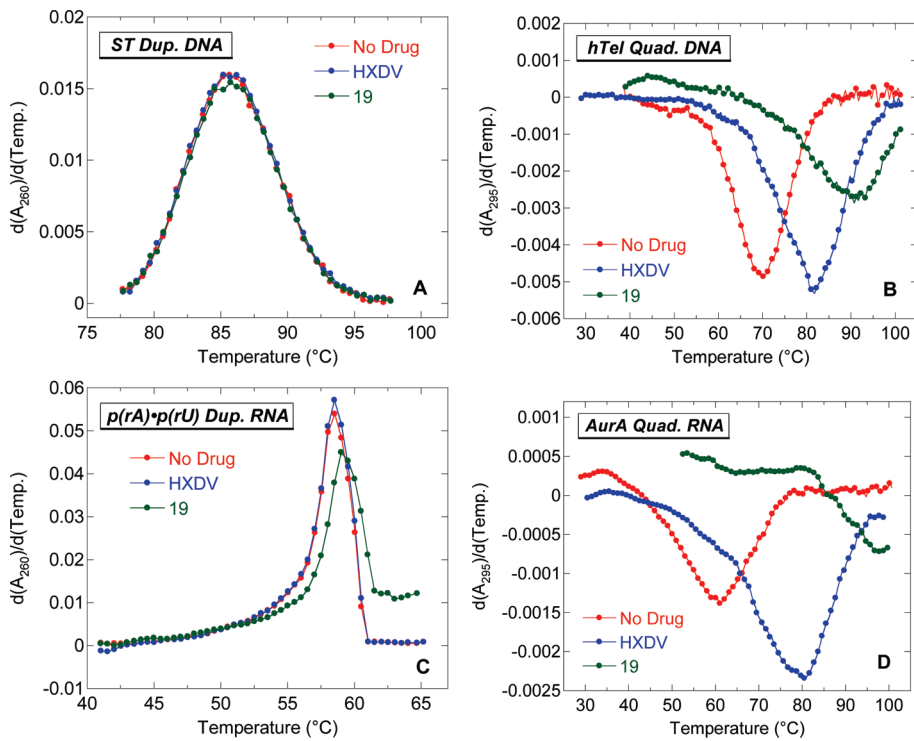


Figure 2. First derivatives of the UV melting profiles of ST duplex DNA (A), hTel quadruplex DNA (B), poly(rA)·poly(rU) duplex RNA (C), and AurA quadruplex RNA (D) in the absence (red) and presence of either HXDV (blue) or **19** (green). The UV melting profiles of the quadruplexes were acquired at 295 nm, while those of the duplexes were acquired at 260 nm. In all experiments, the solution conditions were 10 mM potassium phosphate (pH 7.5) and sufficient KCl (132 mM) to bring the total K⁺ concentration to 150 mM.

Table 2. Impact of HXDV and Various Macrocyclic Pyridyl Polyoxazoles on the Thermal Stabilities of the Duplex and Quadruplex Forms of DNA and RNA

compd	change in thermal stability, ΔT_{tran}^a (°C)			
	ST duplex DNA	poly(rA)·poly(rU) duplex RNA	hTel quadruplex DNA	AurA quadruplex RNA
HXDV	0	0	11.5	19.5
6a	0	0	7.5	ND
11b	0	0	0	ND
18	0	0.5	21.0	ND
19	0	0.5	20.5	37.0

^a ΔT_{tran} reflects the change in transition temperature (T_{tran}) of the target nucleic acid induced by the presence of the compound. Values of T_{tran} were determined from the maxima or minima of first-derivative UV melting profiles exemplified by those shown in Figure 2. The uncertainty in the ΔT_{tran} values is ± 0.5 °C. ND denotes not determined.

quadruplex binding by **11b** may be a consequence of the two thiazole moieties in this compound.

The temperature-induced hypochromic transition at 295 nm exhibited by the AurA RNA sequence in the absence of ligand (see Figure 2D) indicates that this RNA oligomer does indeed adopt a quadruplex structure in the presence of 150 mM K⁺. Moreover, the presence of HXDV and **19** enhance the thermal stability of AurA RNA quadruplex by 19.5 and 37.0 °C, respectively. These ΔT_{tran} values are significantly greater than the corresponding values (11.5 °C for HXDV and 20.5 °C for **19**) associated with the binding of these compounds to the hTel DNA quadruplex. Thus, HXDV and **19** bind to the AurA RNA quadruplex with an even greater affinity than the hTel DNA quadruplex. Our collective UV melting studies indicate that macrocyclic polyoxazoles bind the quadruplex nucleic acid form with a high degree of specificity.

It is of interest to compare the relative extents to which HXDV, **6a**, **11b**, **18**, and **19** bind and stabilize the quadruplex nucleic acid form with their relative cytotoxic potencies. Toward this end, a comparison of the ΔT_{tran} data in Table 2 with the corresponding cytotoxicity (IC₅₀) data in Table 1 reveals a good correlation between cytotoxic potency and quadruplex stabilizing activity.

Compounds that stabilize G-quadruplex conformations of nucleic acids are viewed as a potential novel class of anticancer agents. Many such compounds have been reported, along with their ability to stabilize G-quadruplex DNA in the test tube.⁵ Cytotoxicity data has also been reported for several of these G-quadruplex stabilizers.^{5d,f} Such in vitro studies, however, provide little insight into the ability of G-quadruplex stabilizers to penetrate into cancer cells and to stop the growth and destroy cancer cells in vivo. Telomestatin is one of the few compounds known to stabilize G-quadruplex DNA for which in vivo anticancer activity in a human tumor xenograft has been reported. The results showed that telomestatin does indeed kill such tumor cells in a mouse model.²¹ In comparison with telomestatin, however, the compounds reported in the present study are more selective for stabilizing G-quadruplex DNA. The decision was made to synthesize the 2-(*N,N*-dimethylamino)ethyl substituted analogue **19** on a larger scale and to evaluate its antitumor activity in vivo against a human breast cancer xenograft (MDA-MB-435) in athymic nude mice. The results from the in vivo bioassay of **19** are presented in Figure 3. An experimental group of seven tumor-bearing mice was initially treated with **19** on day 10 and subsequently treated three times a week on alternate days for three weeks at dosing that escalated each week and averaged 32 mg/kg. Despite increasing the dosing from 25 to 42 mg/kg, no significant change in body weight was observed during the three

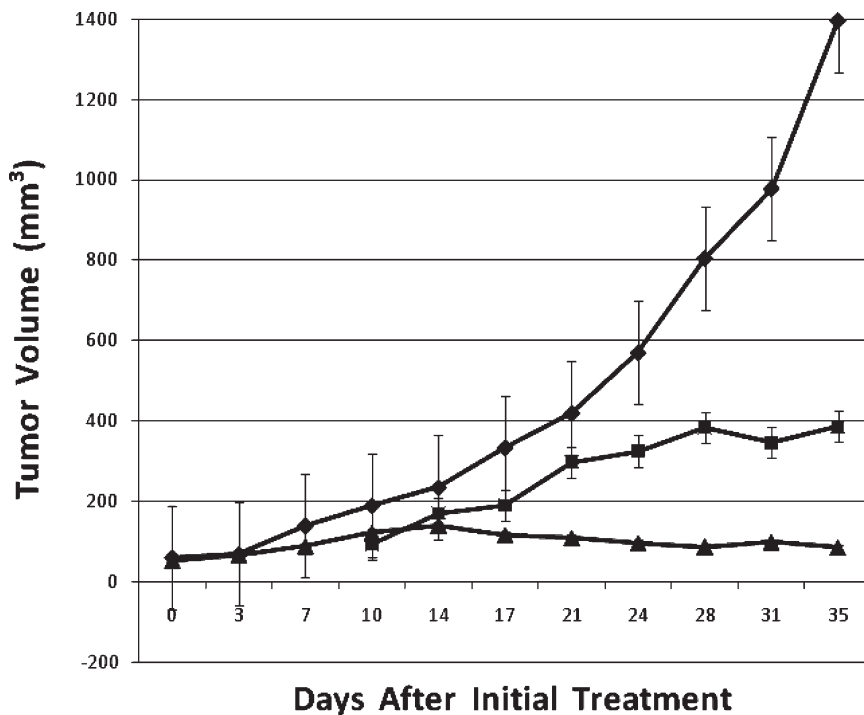


Figure 3. The test compounds, irinotecan (▲), 10 mM citrate (◆), and **19** (■) were administered by ip injection to athymic nude mice with human tumor xenografts established using MDA-MB-435 breast cancer cells. Mice were injected ip 3× weekly. Negative controls (7 mice) were injected with 150 μ L of 10 mM citrate. The positive control group (8 mice) received irinotecan by ip injection at a dose of 20 mg/kg, 3× weekly, for all four weeks. Compound **19** was similarly administered to seven mice, 3× weekly, at a dose of 25 mg/kg starting at week 2 with increasing doses of 32 and 42 mg/kg on weeks 3 and 4, respectively. Data are presented as the mean \pm SE. The % T/C (average tumor volume of treated as compared to control group) is 27.7% for **19** and 6.1% for irinotecan.

Table 3. Average Body Weights of Athymic Nude Mice Treated with Citrate, **19**, and Irinotecan

day	average body weight \pm standard deviation (g)		
	citrate	compd 19	irinotecan
17	22.0 \pm 1.8	19.7 \pm 1.9	19.5 \pm 1.3
24	22.5 \pm 1.5	20.2 \pm 2.3	19.8 \pm 1.4
31	23.9 \pm 1.0	20.9 \pm 2.4	18.4 \pm 2.0 ^a
35	24.6 \pm 1.3 ^b	21.1 \pm 1.9	20.7 \pm 1.6

^a One cage of four mice was found not to have a water bottle, which is reflected in the drop in average weight on day 31. ^b One mouse was euthanized on day 31 because the tumor volume was 2266 mm³, which exceeded protocol limitations.

weeks of treatment, Table 3. The negative control group, which was treated with only citrate buffer, had an average tumor volume > 1350 mm³ after 35 days. In contrast, the tumor-bearing mice treated with **19** had an average tumor volume of < 400 mm³ and had a %T/C value of 27.7%. The positive control group was treated three times a week with irinotecan starting on day 0 at a dose of 20 mg/kg and 35 days after initial treatment had an average tumor volume of < 100 mm³. These results clearly demonstrate the in vivo efficacy of compound **19**.

Conclusions

The results presented above describe an efficient synthesis of pyridyl tetraoxazole platforms that can be performed on a multigram scale. A key feature of these syntheses is the symmetry of the central pyridine, which allows for the use of only a single oxazole building block to rapidly arrive at a difunctional molecule that is elaborated into a macrocycle in only one step. A wide variety of functionalized diamine linkers can be employed for the macrolactamization. Functionality

can also be incorporated on the pyridine ring of the scaffold to allow for the rapid preparation of series of analogues. Of the 17 new macrocycles reported herein, those employing a 1,3-bis(aminomethyl)phenyl linker with a 5-(2-aminoethyl) **18** or a 5-(2-dimethylaminoethyl) substituent **19** displayed the greater cytotoxic potency. These compounds exhibited exquisite selectivity for stabilizing G-quadruplex DNA with no stabilization of duplex DNA or RNA. Compound **19** stabilizes quadruplex mRNA that encodes the cell-cycle checkpoint protein kinase Aurora A. These data may suggest a role for G-quadruplex ligands interacting with mRNA being associated with the biological activity of macrocyclic polyoxazoles. The anticancer activity of **19** was evaluated in vivo against a human breast cancer xenograft (MDA-MB-435) in athymic nude mice. Results from this bioassay indicate that **19** has significant in vivo efficacy as an anticancer agent and administration of doses of **19** increasing from 25 to 42 mg/kg did not result in weight loss or other observable adverse effects in mice. The synthetic methodology outlined will permit more in depth studies on the structure-activity relationships associated with the stabilization of various types of G-quadruplexes. The increased accessibility of test compounds within this series of G-quadruplex stabilizers relative to macrocyclic hexaoxazoles will also allow for expanded studies on the pharmacological properties of these highly selective G-quadruplex stabilizers.

Experimental Section

Chemistry. All reactions were conducted under an atmosphere of argon in oven-dried glassware unless otherwise noted. THF was dried by distillation from sodium-benzophenone. Toluene, CH₂Cl₂, 2,6-lutidine, Et₃N, pyridine, DBU, and CH₃CN were freshly distilled from CaH₂. Anhydrous DMF was obtained by

stirring overnight over anhydrous CuSO_4 , followed by distillation under reduced pressure. All starting materials and reagents were commercially available and were used as received with the exception of 4-bromopyridine-2,6-dicarboxylic acid¹³ (**1b**), 1-bromo-3,5-bis(aminomethyl)benzene¹⁷ (**12**), and 2,6-bis(aminomethyl)pyridine,¹⁵ which were prepared as described previously. Flash chromatography was conducted using 230–400 mesh silica gel obtained from Dynamic Adsorbents, Inc. Melting points were obtained on a Thomas–Hoover apparatus and are uncorrected. Proton (400 MHz) and carbon (125 MHz) NMR spectra were recorded on a Bruker Avance III spectrometer in CDCl_3 unless otherwise noted. Chemical shifts are reported as δ units relative to internal tetramethylsilane. High resolution mass spectra were provided by the Washington University Mass Spectrometry Resource, St. Louis, MO. Each substrate that was evaluated for biological activity was >95% pure as determined by HPLC. All HPLC analyses were performed using a Hewlett-Packard model 1090 system with a YMC CombiScreen C18 column (50 mm \times 4.6 mm). The solvent system was: solvent A (H_2O + 0.5% TFA); solvent B (CH_3CN + 0.1% TFA). Analyses were performed using a program of 10% solvent B for 1 min, a linear gradient of 10–90% solvent B over 10 min, 90% solvent B for 3 min, and then a linear gradient back to 10% solvent B over 5 min with a flow rate of 1.0 mL/min.

Nucleic Acid Molecules. The hTel DNA 24mer (5'-TTGGGT-TAGGGTTAGGGTTAGGG-3') was obtained in its HPLC-purified form from Integrated DNA Technologies, Inc. (Coralville, IA), while the AurA RNA 22mer (5'-AGGGGC-GGCUGGGUCGGAGUGGC-3') was obtained in its PAGE-purified and desalting form from Dharmacon, Inc. (Chicago, IL). The concentrations of all AurA and hTel solutions were determined spectrophotometrically using the following extinction coefficients at 260 nm and 85 °C ($\epsilon_{260-85\text{ }^\circ\text{C}}$) [in units of (mol strand/L)⁻¹·cm⁻¹]: 237500 \pm 4700 for hTel and 236200 \pm 3300 for AurA. These extinction coefficients were determined by enzymatic digestion and subsequent colorimetric phosphate assay using previously established protocols.²² Salmon testes (ST) duplex DNA, as well as the RNA polynucleotides, poly(rA) and poly(rU), were obtained from Sigma (St. Louis, MO) and used without further purification. Polynucleotide solution concentrations were determined using the following extinction coefficients in units of (mol nucleotide/L)⁻¹·cm⁻¹: $\epsilon_{258-25\text{ }^\circ\text{C}} = 9800$ for p(rA) and $\epsilon_{260-25\text{ }^\circ\text{C}} = 9350$ for p(rU).

General Method for Amide Formation. Method A: 2,6-Bis[[1-(4-(methoxycarbonyl)oxazol-2-yl)-2-(trisopropylsilyloxy)ethyl]amino]carbonyl]pyridine (3a). A solution of 2,6-pyridine dicarboxylic acid (418 mg, 2.5 mmol), **2** (1.71 g, 5 mmol), EDC (1.92 g, 10 mmol), and HOBT (1.35 g, 10 mmol) in anhydrous DMF (100 mL) was treated with 2,6-lutidine (2.9 mL, 25 mmol) at 0 °C under argon. The reaction mixture was allowed to warm to room temperature overnight and was then concentrated under reduced pressure. The residue was taken up in a mixture of ethyl acetate and water and the layers were separated. The organic layer was washed sequentially with 5% HCl, water, and brine and then dried over Na_2SO_4 . Upon removal of the solvent and flash chromatography (15–50% EtOAc/hexanes) **3a** was obtained as a pale-yellow oil; 1.6 g (80% yield). ¹H NMR δ 8.54 (d, 2H, $J = 8$), 8.38 (d, 2H, $J = 8$), 8.24 (s, 2H), 8.04 (t, 1H, $J = 7$), 5.62 (dt, 2H, $J = 6, 9$), 4.26 (d, 4H, $J = 7$), 3.90 (s, 6H), 0.96 (m, 42H). ¹³C NMR δ 162.6, 162.4, 147.7, 143.2, 138.1, 132.6, 124.9, 122.4, 63.6, 51.2, 49.3, 16.9, 10.9.

2,6-Bis[[1-(4-(methoxycarbonyl)oxazol-2-yl)-2-(trisopropylsilyloxy)ethyl]amino]carbonyl]-4-bromopyridine (3b). Compound **3b** was prepared from **2** (2.86 g, 8.36 mmol) according to the procedure described for the synthesis of **3a** (method A) using **1b** (1.03 g mg, 4.18 mmol). Bis(amide) **3b** was obtained as a pale-orange oil; 3.47 g (93% yield). ¹H NMR δ 8.50 (m, 4H), 8.24 (s, 2H), 5.59 (dt, 2H, $J = 3, 6$), 4.25 (d, 4H, $J = 6$), 3.85 (s, 6H), 0.90 (m, 42H). ¹³C NMR δ 162.1, 161.5, 156.2, 148.6, 143.3, 135.3, 132.6, 128.3, 63.4, 51.2, 49.4, 16.9, 11.0.

General Method for the Synthesis of Oxazoles. Method B: 2,6-Bis[4-[(4-methoxycarbonyl)oxazol-2-yl]oxazol-2-yl]pyridine (4a). TIPS ether **3a** (750 mg, 0.92 mmol) was dissolved in a mixture of anhydrous THF (20 mL) and pyridine (2 mL) and HF–pyridine complex (0.5 mL) was added. The reaction was stirred at room temperature (drying tube) overnight and a white solid precipitated. A saturated aqueous solution of NaHCO_3 was added, whereupon additional precipitate formed and was filtered. The solids were washed with water, and the filtrate was then extracted with CH_2Cl_2 . The organic phase was separated, dried over Na_2SO_4 , and concentrated in vacuo to a white solid. This was combined with the filtered solid to give the diol as a white solid; 463 mg (100% yield); mp 218–220 °C. ¹H NMR ($\text{DMSO}-d_6$) δ 9.58 (d, 2H, $J = 8$), 8.84 (s, 2H), 8.24 (m, 3H), 5.29 (m, 2H), 4.04 (m, 4H), 3.79 (s, 6H). ¹³C NMR ($\text{DMSO}-d_6$) δ 163.3, 162.7, 160.9, 148.2, 145.4, 132.1, 125.1, 60.8, 51.6, 50.0. IR (Nujol) 3500, 3364, 3287, 1732 cm^{-1} .

The diol (463 mg, 0.92 mmol) was suspended in anhydrous CH_2Cl_2 (30 mL) and placed under argon. After cooling to –78 °C, DAST (0.3 mL, 2.3 mmol) was added and the reaction was stirred for 4 h at that temperature. Solid potassium carbonate (317 mg, 2.3 mmol) was added and the reaction mixture warmed slightly and was poured into saturated NaHCO_3 and extracted with CH_2Cl_2 . The organic extracts were dried over Na_2SO_4 and concentrated under reduced pressure to give the bis(oxazoline) as a white solid; 428 mg (99.5% yield); mp 214–217 °C. ¹H NMR (CD_3OD) δ 8.36 (s, 2H), 8.26 (d, 2H, $J = 8$), 8.01 (t, 1H, $J = 8$), 5.67 (t, 2H, $J = 9$), 4.97 (d, 4H, $J = 8$), 4.28 (s, 6H). ¹³C NMR (CD_3OD) δ 165.5, 163.1, 161.5, 146.0, 145.1, 138.0, 133.3, 126.9, 71.4, 63.7, 52.1.

The bis(oxazoline) (428 mg, 0.92 mmol) was suspended in anhydrous CH_3CN (40 mL) and placed under argon. After cooling to 0 °C, the magnetically stirred solution was treated dropwise with DBU (0.55 mL, 3.68 mmol) and then BrCCl_3 (0.44 mL, 4.42 mmol). The reaction was allowed to warm to room temperature overnight and a white precipitate formed. The precipitate was filtered and washed with CH_2Cl_2 to give **4a** as a white solid; 341 mg (80% yield); mp >220 °C (dec). ¹H NMR δ 8.59 (s, 2H), 8.44 (d, 2H, $J = 8$), 8.37 (s, 2H), 8.08 (t, 1H, $J = 8$), 3.98 (s, 6H).

2,6-Bis[4-[(4-methoxycarbonyl)oxazol-2-yl]oxazol-2-yl]-4-bromopyridine (4b). Compound **4b** was prepared from **3b** using method B. Thus, **3b** (910 mg, 1.02 mmol) afforded 282 mg of **3b** (71% overall yield for the three steps) as a white solid; mp 280–282 °C (dec). ¹H NMR δ 8.63 (s, 2H), 8.60 (s, 2H), 8.37 (s, 2H), 3.83 (s, 6H).

General Method for Ester Hydrolysis to Form Pyridyl Tetraoxazole Scaffolds. Method C: 2,6-Bis[4-(4-carboxyoxazol-2-yl)-oxazol-2-yl]pyridine (5a). Diester **4a** (150 mg, 0.32 mmol) was suspended in THF (50 mL) and H_2O (15 mL) and treated with LiOH (30 mg, 0.71 mmol). The mixture was heated to 80 °C overnight and was then cooled to room temperature. THF was removed by rotary evaporator, and the residue was treated with 5% HCl. A white precipitate formed and was filtered and washed with water to give **5a** as a white solid; 140 mg (100% yield); mp 315–318 °C (dec). ¹H NMR ($\text{DMSO}-d_6$) δ 9.00 (s, 2H), 8.52 (s, 2H), 8.15 (m, 3H). IR (Nujol) 3418–2719 (br), 1727 cm^{-1} .

2,6-Bis[4-(4-carboxyoxazol-2-yl)oxazol-2-yl]-4-bromopyridine (5b). Compound **4b** (54 mg, 0.1 mmol) and LiBr (9 mg, 0.1 mmol) were suspended in THF (10 mL) and water (0.5 mL), and the mixture was then placed under argon. To this was added DBU (60 μL , 0.4 mmol), and the mixture was heated at reflux overnight. After cooling to room temperature, solvents were removed under reduced pressure and the residue was treated with 1N HCl to give a white solid. This was filtered and washed with water and then CH_2Cl_2 to give **5b** as a white solid; 47 mg (100% yield); mp 205–206 °C (dec). ¹H NMR (DMSO) δ 9.19 (s, 2H), 8.90 (s, 2H), 8.48 (s, 2H). IR (thin film) 3390–2516 (br), 1727 cm^{-1} .

General Method for Macrocyclization. Method D: Pyridine Tetraoxazole Macrocycle with a 1,3-Bis(aminomethyl)phenyl Linker (6a). Diacid **5a** (28 mg, 0.065 mmol), EDC (50 mg, 0.26 mmol), and HOBT (35 mg, 0.26 mmol) were dissolved in

anhydrous DMF (120 mL) at room temperature under argon. The diamine linker, in this case 1,3-bis(aminomethyl)benzene (8.5 μ L 0.065 mmol) in DMF (0.5 mL) and 2,6-lutidine (45 μ L, 0.39 mmol) were added and the reaction was stirred at room temperature for 2 d. Solvent was removed under reduced pressure, and the resulting residue was triturated with water. A white precipitate formed and was filtered, collected, and purified by flash chromatography eluting with 1–5% MeOH/CH₂Cl₂. Macrocycle **6a** was isolated as a white solid; 10 mg (30%), mp 320–324 $^{\circ}$ C (dec). ¹H NMR (CDCl₃ + CD₃OD) δ 8.34 (d, 4H, *J* = 5), 8.11, (s, 3H), 7.58 (s, 1H), 7.33 (m, 3H), 4.62 (s, 4H). ¹³C NMR (CDCl₃ + CD₃OD) δ 159.8, 159.3, 153.3, 144.1, 140.5, 138.5, 138.0, 136.8, 136.6, 130.7, 129.3, 128.5, 128.1, 121.9, 42.8. HRMS (ESI) *m/z* calcd for C₂₇H₁₈N₇O₆ (M + H) 536.1368; found 536.1343.

4-Bromopyridine Tetraoxazole Macrocycle with a 1,3-Bis(aminomethyl)phenyl Linker (6b). Using method D, **5b** (43 mg, 0.1 mmol) was macrocyclized with 1,3-bis(aminomethyl)benzene (13 μ L, 0.1 mmol). The product, **6b** was obtained as a white solid; 18 mg (35%); mp 211–213 $^{\circ}$ C. ¹H NMR (CDCl₃ + CD₃OD) δ 8.37 (s, 2H), 8.32 (m, 2H), 8.26 (s, 2H), 7.36 (s, 3H), 4.61 (s, 4H). ¹³C NMR (CDCl₃ + CD₃OD) δ 160.2, 159.7, 154.2, 146.1, 141.5, 139.8, 137.7, 137.4, 132.0, 130.2, 129.7, 129.4, 126.1, 108.0, 43.9. HRMS (ESI) *m/z* calcd for C₂₇H₁₇BrN₇O₆ (M + H) 614.0424; found 614.0420.

Pyridine Tetraoxazole Macrocycle with a 2,6-Bis(aminomethyl)-pyridyl Linker (7a). Using method D, **5a** (40 mg, 0.092 mmol) was macrocyclized with 2,6-bis(aminomethyl)pyridine¹⁵ (13 mg, 0.092 mmol). The product, **7a** was obtained as a white solid; 11 mg (22%); mp 330 $^{\circ}$ C (dec). ¹H NMR (CDCl₃ + CD₃OD) δ 8.33 (s, 4H), 8.09 (s, 3H), 7.72 (t, 1H, *J* = 8), 7.40 (d, 2H, *J* = 8), 4.76 (s, 4H). ¹³C NMR (CDCl₃ + CD₃OD) δ 159.8, 159.5, 144.3, 140.4, 138.3, 137.8, 137.4, 136.4, 130.8, 122.5, 121.7, 71.2. HRMS (ESI) *m/z* calcd for C₂₆H₁₇N₈O₆ (M + H) 537.1271; found 537.1252.

General Method for Macrocyclization. Method E: Pyridine Tetraoxazole Macrocycle with a Bis(2-aminoethyl)amine Linker (8). A solution of **5a** (23 mg, 0.053 mmol) and copper(II) triflate (19 mg, 0.053 mmol) in anhydrous DMF (100 mL) was stirred under argon at room temperature for 3 h. At that point, EDC (41 mg, 0.21 mmol) and HOBT (29 mg, 0.21 mmol) were added and the color of the solution immediately became bright yellow. The solution was cooled to 0 $^{\circ}$ C and 2,6-lutidine (37 μ L, 0.32 mmol) was added, followed by a solution of diethylenetriamine (6 μ L, 0.053 mmol) in 0.5 mL of DMF, which was added by syringe pump over 30 min. The reaction was stirred at room temperature, and the color gradually changed to pale blue. After 2 d, solvent was removed under reduced pressure and the residue was triturated with water to give a white precipitate that was filtered and subjected to flash chromatography eluting with 1–5% MeOH/CH₂Cl₂ to give **8** as a white solid; 4 mg (15% yield); mp 276 $^{\circ}$ C (dec). ¹H NMR (CDCl₃ + CD₃OD) δ 8.47 (s, 2H), 8.37 (s, 2H), 8.19 (s, 3H), 3.98 (m, 4H) 3.35 (m, 4H). HRMS (ESI) *m/z* calcd for C₂₃H₁₉N₈O₆ (M + H) 503.1428; found 503.1413.

2-[[1-(4-(Methoxycarbonyl)oxazol-2-yl)-2-(trisopropylsilyloxy)-ethyl]amino]thiocarbonyl]-6-[[1-(4-(methoxycarbonyl)oxazol-2-yl)-2-(trisopropylsilyloxy)ethyl]amino]carbonyl]pyridine (9a). A solution of **3a** (100 mg, 0.122 mmol) in toluene (10 mL) was treated with Lawesson's reagent (50 mg, 0.12 mmol) under argon and heated at 80 $^{\circ}$ C for 4 h. The reaction mixture was then allowed to cool to room temperature, and toluene was removed by rotary evaporator. The residue was purified by flash chromatography eluting with 5–25% EtOAc/hexanes to afford **9a** as a yellow oil; 54 mg (53% yield). ¹H NMR δ 10.46 (d, 1H, *J* = 8), 8.82, (dd, 1H, *J* = 1, 9), 8.62 (d, 1H, *J* = 8), 8.36 (dd, 1H, *J* = 1, 8), 8.31 (s, 1H), 8.23 (s, 1H), 8.00 (t, 1H, *J* = 6), 6.19 (dt, 1H, *J* = 3, 5), 5.61 (dt, 1H, *J* = 2, 6), 4.38 (d, 2H, *J* = 5), 4.26 (d, 2H, 6), 3.88 (s, 6H), 0.95 (m, 42H). ¹³C NMR δ 190.7, 170.3, 162.7, 162.6, 161.6, 160.4, 146.5, 143.5, 143.2, 137.7, 133.0, 127.5, 124.6, 62.6, 54.7, 51.2, 49.4.

2,6-Bis[[1-(4-(methoxycarbonyl)oxazol-2-yl)-2-(trisopropylsilyloxy)ethyl]amino]thiocarbonyl]-pyridine (9b). A solution of **3a** (100 mg, 0.122 mmol) in toluene (10 mL) was treated with Lawesson's reagent (149 mg, 0.37 mmol) under argon and heated at 80 $^{\circ}$ C for 4 h. The reaction mixture was then allowed to cool to room temperature, and toluene was removed by rotary evaporator. The residue was purified by flash chromatography eluting with 5–25% EtOAc/hexanes to afford **9b** as a yellow oil; 91 mg (88% yield). ¹H NMR δ 10.26 (d, 2H, *J* = 8), 8.79 (d, 2H, *J* = 8), 8.29 (s, 2H), 7.97 (t, 1H, *J* = 8), 6.18 (dt, 2H, *J* = 3, 6), 4.37 (m, 4H), 3.88 (s, 6H), 1.00 (m, 42H). ¹³C NMR δ 190.9, 161.5, 160.3, 148.7, 143.5, 137.4, 132.6, 127.1, 62.6, 54.7, 51.2, 16.8, 10.9.

2-[4-[(4-Methoxycarbonyl)oxazol-2-yl]thiazol-2-yl]-6-[4-[(4-methoxycarbonyl)oxazol-2-yl]oxazol-2-yl]pyridine (10a). Compound **10a** was prepared from **9a** (138 mg, 0.166 mmol) using method B. The yield of **10a** for the three-step procedure was 57 mg (72%); cream-colored solid; mp 305–310 $^{\circ}$ C (dec). ¹H NMR (CDCl₃ + CD₃OD) δ 8.62 (s, 1H), 8.49 (d, 1H, *J* = 7), 8.35 (m, 4H), 8.06 (m, 1H), 3.98 (s, 6H).

2,6-Bis[4-[(4-methoxycarbonyl)oxazol-2-yl]thiazol-2-yl]pyridine (10b). Compound **10b** was prepared from **9b** (91 mg, 0.11 mmol) using method B. The yield of **10b** for the three-step procedure was 28 mg (52%); brown solid; mp 330–333 $^{\circ}$ C (dec). ¹H NMR (DMSO-d₆) δ 9.10 (s, 2H), 8.80 (d, 2H, *J* = 8), 8.72 (s, 2H) 8.33 (t, 1H, *J* = 8), 3.93 (s, 6H).

Pyridine Mono(thiazole) Tris(oxazole) Macrocycle with a 1,3-Bis(aminomethyl)phenyl Linker (11a). Diester **10a** (57 mg, 0.12 mmol) was hydrolyzed to the corresponding diacid in 78% yield using method C. Macrocyclization of a portion of the diacid (23 mg, 0.051 mmol) with 1,3-bis(aminomethyl)benzene (7 μ L, 0.051 mmol) using method E afforded **11a** as white solid; 9 mg (33% yield); mp 245 $^{\circ}$ C. ¹H NMR δ 8.31 (s, 1H), 8.28 (s, 1H), 8.26 (s, 1H), 8.00 (m, 4H), 7.37 (m, 4H), 4.62, (m, 4H). ¹³C NMR δ 140.0, 139.7, 138.4, 137.9, 136.7, 128.8, 128.3, 127.8, 127.4 123.1, 121.9, 120.6, 113.4, 42.9, 42.3. HRMS (ESI) *m/z* calcd for C₂₇H₁₈N₇O₅S (M + H) 552.1085; found 552.1086.

Pyridine Bis(thiazole) Bis(oxazole) Macrocycle with a 1,3-Bis(aminomethyl)phenyl Linker (11b). Diester **10b** (52 mg, 0.11 mmol) was hydrolyzed to the corresponding diacid in quantitative yield using method C. A portion of the diacid (21 mg, 0.045 mmol) was dissolved in dry DMF (30 mL) and treated with EDC (17 mg, 0.09 mmol) and HOBT (12 mg, 0.09 mmol) and cooled to 0 $^{\circ}$ C under argon. To this was added 2,6-lutidine (26 μ L, 0.23 mmol) and 1-(*N*-Boc-aminomethyl)-3-(aminomethyl)benzene (11 μ L, 0.045 mmol), and the solution was allowed to warm to room temperature overnight. Solvents were removed under reduced pressure, and the residue was extracted with EtOAc. The organic solution was washed with brine and dried over Na₂SO₄, filtered, and evaporated to give 34 mg of crude product. This was dissolved in CH₂Cl₂ (3 mL), cooled to 0 $^{\circ}$ C, and treated with TFA (3 mL). After stirring at 0 $^{\circ}$ C for 2 h solvents were removed under reduced pressure to give the free amine as its TFA salt (25 mg, 68% yield). Macrolactamization using method D gave product **11b** as white solid; 6 mg (43% yield); mp 274–275 $^{\circ}$ C (dec). ¹H NMR (CDCl₃ + CD₃OD) δ 8.38 (m, 4H), 8.42 (s, 2H), 7.97 (m, 2H), 7.30 (m, 3H), 4.63 (d, 4H, *J* = 6). ¹³C NMR (CDCl₃ + CD₃OD) δ 140.7, 137.4, 136.0, 128.4, 126.6, 126.5, 123.2, 120.5, 42.6. HRMS (ESI) *m/z* calcd for C₂₇H₁₈N₇O₄S₂ (M + H) 568.0863; found 568.0864.

Pyridine Tetraoxazole Macrocycle with a 1,3-Bis(aminomethyl)-5-bromophenyl Linker (13a). Using method D, **5a** (43 mg, 0.1 mmol) was macrocyclized with 1-bromo-3,5-bis(aminomethyl)-benzene dihydrochloride **12**¹⁷ (21 mg, 0.073 mmol). The product, **13a** was obtained as a white solid; 26 mg (58%); mp 248–250 $^{\circ}$ C. ¹H NMR δ 8.28 (s, 2H), 8.25(s, 2H), 8.08 (m, 3H), 7.51 (m, 3H), 7.29 (m, 2H), 4.56 (d, 4H, *J* = 5). ¹³C NMR δ 159.9, 159.3, 153.0, 144.3, 140.1, 138.5, 138.0, 136.7, 136.6, 130.7, 128.3, 126.0, 122.5, 42.9. HRMS (ESI) *m/z* calcd for C₂₇H₁₇BrN₇O₆ (M + H) 614.0418; found 614.0418.

4-Bromopyridine Tetraoxazole Macrocycle with a 1,3-Bis(aminomethyl)-5-bromophenyl Linker (13b). Using method D, **5b** (17 mg, 0.033 mmol) was macrocyclized with **12** (10 mg, 0.033 mmol). The product, **13b** was obtained as a white solid; 5 mg (22%); mp 250 °C (dec). ¹H NMR (CDCl₃ + CD₃OD) δ 8.28 (s, 2H), 8.22 (s, 2H), 8.15 (s, 2H), 7.39 (s, 3H), 4.46 (s, 4H). ¹³C NMR (CDCl₃ + CD₃OD) δ 160.3, 159.6, 145.7, 141.6, 139.8, 139.7, 131.7, 131.6, 128.4, 125.9, 122.7, 43.0. HRMS (ESI) *m/z* calcd for C₂₇H₁₆Br₂N₇O₆ (M + H) 691.9529; found 691.9546.

5-[2-(Benzylloxycarbonylamino)ethyl]-1,3-bis([*tert*-butyloxycarbonylamino)methyl]benzene (14a). A solution of **12** (2.04 g, 9.5 mmol), di-*tert*-butyl dicarbonate (4.35 g, 19.9 mmol), and triethylamine (2.9 mL, 20.8 mmol) in anhydrous CH₂Cl₂ (25 mL) was stirred overnight under argon. The reaction mixture was poured into 5% HCl and extracted with CH₂Cl₂. The organic layer was dried over Na₂SO₄, filtered, and concentrated. Flash chromatography eluting with 10–40% EtOAc/hexanes gave the di-Boc derivative as a white solid; 2.51 g (63% yield). ¹H NMR δ 7.32 (s, 2H), 7.11 (s, 1H), 4.86 (s, 2H), 4.28 (d, 4H, *J* = 4), 1.46 (18H). ¹³C NMR δ 154.8, 141.6, 129.2, 124.9, 122.9, 79.9, 44.0, 28.4.

A portion of the di-Boc derivative (209 mg, 0.5 mmol), potassium 2-(benzylloxycarbonylamino)ethyltrifluoroborate¹⁸ (186 mg, 0.76 mmol), Cs₂CO₃ (429 mg, 1.5 mmol), and PdCl₂-(dppf)·CH₂Cl₂ (21 mg, 0.025 mmol) were dissolved in toluene (15 mL) and water (5 mL) was added. The flask was purged with argon and heated to 80 °C for 17.5 h. After cooling to room temperature, the mixture was poured into saturated NH₄Cl and extracted with CH₂Cl₂. The organic layer was dried over Na₂SO₄, concentrated, and purified by flash chromatography eluting with 10–50% EtOAc/hexanes. The coupled product **14a** was obtained as a colorless oil; 205 mg (79% yield). ¹H NMR δ 7.32 (m, 5H), 7.04 (s, 1H), 6.98 (s, 2H), 5.09 (s, 2H), 4.82 (m, 3H), 4.26 (d, 4H, *J* = 4), 3.42 (m, 2H), 2.78 (m, 2H), 1.46 (s, 18H). ¹³C NMR δ 156.3, 155.9, 139.8, 139.5, 136.6, 128.5, 128.1, 126.8, 124.6, 79.6, 66.7, 44.5, 42.1, 36.0, 28.4.

5-[2-(Benzylloxycarbonylamino)ethyl]-1,3-bis(aminomethyl)-benzene (14b). A solution of **14a** (205 mg, 0.4 mmol) in CH₂Cl₂ (1 mL) and anisole (1 mL) and cooled to 0 °C. TFA (1 mL) was added and the solution was stirred at 0 °C for 3.75 h. The solution was evaporated under reduced pressure, and residual anisole was removed azeotropically with benzene. The product was dissolved in MeOH and stirred for several minutes with IRA-400 resin. The resin was filtered and washed several times with MeOH. Upon evaporation of the solvent, diamine **14b** was obtained as a white solid; 125 mg (100% yield). ¹H NMR δ 7.34 (m, 5H), 7.13 (s, 1H), 7.01 (s, 2H), 5.10 (s, 2H), 4.80 (s, 1H), 3.84 (s, 4H), 3.46 (m, 2H), 2.81 (m, 2H), 1.48 (br s, 4H). ¹³C NMR δ 156.3, 144.0, 136.6, 128.5, 128.2, 126.0, 124.1, 66.7, 46.4, 42.2, 36.1.

Pyridine Tetraoxazole Macrocycle with a 5-[2-(Benzylloxycarbonylamino)ethyl]-1,3-bis(aminomethyl)phenyl linker (15a). Using method D, **5a** (50 mg, 0.11 mmol) was macrocyclized with **14b** (36 mg, 0.11 mmol). The product, **15a** was obtained as a white solid; 33 mg (42%); mp 196–198 °C. ¹H NMR (CDCl₃ + CD₃OD) δ 8.41 (d, 2H, *J* = 4), 8.34 (s, 2H), 8.32 (s, 2H), 8.10 (s, 3H), 7.42 (s, 1H), 7.30 (m, 5H), 7.18 (s, 2H), 5.37 (s, 1H), 5.04 (s, 2H), 4.59 (d, 4H, *J* = 4), 3.41 (m, 4H). ¹³C NMR (CDCl₃ + CD₃OD) δ 160.9, 160.4, 156.8, 156.7, 154.3, 145.1, 141.5, 140.4, 139.5, 139.0, 138.1, 137.6, 136.8, 131.7, 129.6, 128.5, 128.2, 128.0, 127.9, 122.9, 66.6, 42.2, 35.9. HRMS (ESI) *m/z* calcd for C₃₇H₂₉N₈O₈ (M + H) 713.2108; found 713.2091.

4-Bromopyridine Tetraoxazole Macrocycle with a 5-[2-(Benzylloxycarbonylamino)ethyl]-1,3-bis(aminomethyl)phenyl Linker (15b). Using method D, **5b** (20 mg, 0.039 mmol) was macrocyclized with **14b** (12 mg, 0.039 mmol). The product, **15b**, was obtained as a white solid; 13 mg (42%); mp 204–205 °C. ¹H NMR δ 8.24 (m, 5H), 7.65 (s, 2H), 7.56 (m, 2H), 7.3 (m, 5H), 7.17 (s, 2H), 5.06 (s, 2H), 4.91 (s, 1H), 4.56 (s, 2H), 3.44 (m, 2H), 2.80 (m, 2H). ¹³C NMR δ 159.6, 159.4, 159.4, 156.3, 154.0, 153.9, 147.6, 146.2, 140.8,

139.4, 138.1, 137.5, 136.7, 134.9, 132.1, 132.0, 130.0, 129.9, 128.5, 128.4, 128.3, 127.9, 127.7, 125.9, 125.9, 121.1, 108.2, 107.8, 66.5, 43.8, 42.2, 35.9. HRMS (ESI) *m/z* calcd for C₃₇H₂₈BrN₈O₈ (M + H) 791.1213; found 791.1199.

N-(3,5-Bis(aminomethyl)phenethyl)-2,2-trifluoroacetamide (16). A solution of **14a** (62 mg, 0.13 mmol) in EtOH (10 mL) was treated with 20% Pd(OH)₂/C (10 mg) and stirred under 1 atm H₂ (balloon) for 21 h. The catalyst was filtered and washed with EtOH to afford the primary phenethylamine as a colorless oil; 50 mg (100% yield). ¹H NMR δ 7.02 (m, 3H), 4.94 (s, 2H), 4.27 (d, 4H, *J* = 8), 2.94 (m, 2H), 2.71 (m, 2H), 1.47 (s, 18H). ¹³C NMR δ 155.9, 140.7, 139.6, 126.9, 124.3, 79.5, 44.5, 43.4, 39.9, 28.4.

A portion of the amine (37 mg, 0.097 mmol) was dissolved in a solution of pyridine (3 mL) and trifluoroacetic anhydride (2 mL) and stirred at room temperature under a drying tube for 19 h. The reaction mixture was diluted with CH₂Cl₂ and washed with 5% HCl. The aqueous layer was back-extracted with CH₂Cl₂ (3 × 20 mL), and the combined organic layers were washed with 5% HCl and then dried over Na₂SO₄. After concentration, flash chromatography (10–40% EtOAc/hexanes) afforded the trifluoroacetamide as a pale-yellow oil; 42 mg (91% yield). ¹H NMR δ 7.06 (s, 1H), 6.98 (s, 2H), 6.82 (s, 1H), 4.96 (s, 2H), 4.25 (d, 4H, *J* = 8), 3.55 (m, 2H), 2.84 (m, 2H), 1.46 (s, 18H). ¹³C NMR δ 157.8, 157.5, 157.1, 156.7, 156.0, 140.1, 138.6, 126.7, 124.9, 117.3, 114.4, 79.7, 44.4, 40.9, 34.8, 28.4.

The Boc groups were removed by dissolving the trifluoroacetamide (63 mg, 0.13 mmol) in dry CH₂Cl₂ (2 mL), cooling to 0 °C under argon, and adding TFA (1 mL). After 1.5 h solvent was removed under reduced pressure to give **16** as a pale-yellow oil; 65 mg (100% yield). ¹H NMR δ 7.34 (s, 1H), 7.31 (s, 2H), 5.92 (s, 1H), 4.00 (s, 4H), 3.54 (m, 2H), 2.88 (m, 2H). ¹³C NMR δ 139.9, 137.3, 128.5, 126.0, 47.8, 43.6, 32.8.

Pyridine Tetraoxazole Macrocycle with a 5-[2-(Trifluoroacetamido)ethyl]-1,3-bis(aminomethyl)phenyl Linker (17). Using method D, **5a** (44 mg, 0.1 mmol) was macrocyclized with **16** (51 mg, 0.1 mmol). The product, **17**, was obtained as a white solid; 21 mg (31% yield); mp 290 °C (dec). ¹H NMR (CDCl₃ + CD₃OD) δ 8.38 (s, 2H), 8.37 (s, 2H), 8.12 (s, 2H) 7.60 (s, 1H), 7.47 (s, 1H), 7.19 (s, 2H), 4.60 (s, 4H), 4.07 (m, 2H), 3.40 (m, 2H). ¹³C NMR (CDCl₃ + CD₃OD) δ 160.9, 154.1, 145.0, 141.6, 140.0, 139.5, 138.2, 137.6, 131.6, 129.7, 128.6, 122.9, 43.7, 38.8, 34.1. HRMS (ESI) *m/z* calcd for C₃₁H₂₂F₃N₈O₇ (M + H) 675.1564; found 675.1546.

Pyridine Tetraoxazole Macrocycle with a 5-(2-Aminoethyl)-1,3-bis(aminomethyl)phenyl Linker (18). A suspension of **17** (15 mg, 0.02 mmol) and K₂CO₃ (17 mg, 0.12 mmol) in MeOH (10 mL) was heated at reflux for 4.75 h. After cooling to room temperature, solvent was removed under reduced pressure and the residue was partitioned between water and CH₂Cl₂. The organic layer was separated and dried over Na₂SO₄, filtered, and evaporated to give **18** as a white solid; 10.5 mg (81% yield); mp 277–280 °C (dec). ¹H NMR (CDCl₃ + CD₃OD) δ 8.42 (s, 2H), 8.40 (s, 2H), 8.13 (s, 3H), 7.45 (s, 1H), 7.19 (s, 2H), 4.60 (s, 4H), 2.92 (m, 2H), 2.75 (m, 2H). ¹³C NMR (CDCl₃ + CD₃OD) δ 161.0, 160.5, 154.4, 145.1, 141.7, 140.9, 139.7, 139.2, 138.1, 137.6, 131.7, 129.5, 129.2, 128.9, 123.0, 43.8, 43.0, 39.4. HRMS (ESI) *m/z* calcd for C₂₉H₂₃N₈O₆ (M + H) 579.1741; found 579.1723.

Pyridine Tetraoxazole Macrocycle with a 5-[2-(*N*-Dimethylamino)ethyl]-1,3-bis(aminomethyl)phenyl Linker (19). Primary amine **18** (6 mg, 0.01 mmol) was dissolved in 1:4 MeOH/CH₂Cl₂ (5 mL) and placed under argon. A solution of 37% aqueous formaldehyde (0.25 mL) was added, and the reaction mixture was allowed to stir at room temperature for 10 min. At that point, sodium triacetoxylborohydride (15 mg, 0.07 mmol) was added and stirring continued for 16 h. The reaction was not complete by TLC, and additional formaldehyde solution (0.25 mL) and NaBH(OAc)₃ (15 mg) was added. After 6 h, TLC showed the reaction to be complete and it was poured into saturated NaHCO₃ and extracted with CH₂Cl₂. After concentrating,

flash chromatography (1–15% MeOH/CH₂Cl₂) afforded **19** as a white solid; 6 mg (100% yield); 295 °C (dec). ¹H NMR (CDCl₃ + CD₃OD) δ 8.34 (s, 2H), 8.33 (s, 2H), 8.10 (s, 3H), 7.41 (s, 1H), 7.19 (s, 2H), 4.59 (s, 4H), 2.79 (m, 2H), 2.61 (m, 2H), 2.30 (s, 6H). ¹³C NMR (CDCl₃ + CD₃OD) δ 160.8, 160.3, 154.2, 145.1, 141.5, 139.4, 139.0, 137.9, 131.7, 129.4, 128.1, 122.8, 45.0, 43.8. HRMS (ESI) *m/z* calcd for C₃₁H₂₇N₈O₆ (M + H) 607.2054; found 607.2029.

2,6-Bis[[1-(4-(methoxycarbonyl)oxazol-2-yl)-2-(trisopropylsilyloxy)ethyl]amino]carbonyl-4-hydroxypyridine (20). Using method A, chelidonic acid (230 mg, 1.26 mmol) was condensed with **2** (860 mg, 2.51 mmol). The product, **20** was obtained as a yellow oil; 900 mg (86% yield). ¹H NMR δ 10.62 (s, 1H), 8.70 (d, 2H, *J* = 9), 8.25 (s, 2H), 7.82 (s, 2H), 5.57 (m, 2H), 4.24 (d, 4H, *J* = 6), 3.90 (s, 6H), 0.96 (m, 42H). ¹³C NMR δ 165.9, 163.0, 162.0, 160.4, 149.2, 143.2, 132.4, 112.6, 63.5, 51.2, 49.2, 16.8, 10.9.

2,6-Bis[[1-(4-(methoxycarbonyl)oxazol-2-yl)-2-(trisopropylsilyloxy)ethyl]amino]carbonyl-4-[(3-phthalimidopropyl)oxy]pyridine (21). A solution of **20** (642 mg, 0.77 mmol) and *N*-(3-bromopropyl)phthalimide (227 mg, 0.85 mmol) in anhydrous DMF (10 mL) was treated with DBU (0.13 mL, 0.85 mmol) and warmed to 60 °C for 6 h. After cooling to room temperature, the reaction mixture was poured into water and extracted with EtOAc. The organic phase was washed with 5% HCl and then brine and then dried over Na₂SO₄. Flash chromatography (1–4% MeOH/CH₂Cl₂) afforded **21** as a colorless oil; 727 mg (92% yield). ¹H NMR δ 8.61 (d, 2H, *J* = 9), 8.24 (s, 2H), 7.84 (m, 2H), 7.73 (m, 4H), 5.59 (m, 2H), 4.23 (m, 6H), 3.93 (m, 8H), 2.25 (m, 2H), 1.03 (m, 42H). ¹³C NMR δ 167.4, 166.4, 162.5, 162.3, 160.5, 149.5, 143.3, 133.2, 132.6, 131.2, 122.5, 111.1, 65.7, 63.5, 51.2, 49.3, 34.2, 27.0, 16.9, 10.9.

2,6-Bis[4-(4-carboxyoxazol-2-yl)oxazol-2-yl]-4-[(3-phthalimidopropyl)oxy]pyridine (22). Using method B, **21** (1.05 g, 1.03 mmol) was deprotected, cyclodehydrated, and converted into the pyridyl tetraoxazole diester, a white solid; 470 mg (68% yield for the three steps); ¹H NMR (DMSO-*d*₆) δ 9.16 (s, 2H), 9.02 (s, 2H), 7.82 (m, 4H), 7.61 (s, 2H), 4.37 (t, 2H, *J* = 6), 3.81 (t, 2H, *J* = 6), 2.14 (m, 2H).

A portion of this material (150 mg, 0.23 mmol) was dissolved in DMF (5 mL) and treated with LiCl (95 mg, 2.3 mmol) at reflux overnight. After cooling to room temperature, DMF was removed under reduced pressure. Addition of 1N HCl to the residue formed a precipitate that was filtered and washed with water to give **22** as a white solid; 144 mg (100% yield); mp 147–150 °C. ¹H NMR (DMSO-*d*₆) δ 9.14 (s, 2H), 8.90 (s, 2H), 7.82 (m, 4H), 7.62 (s, 2H), 4.37 (t, 2H, *J* = 6), 3.81 (t, 2H, *J* = 6), 2.14 (m, 2H).

4-[(3-Phthalimidopropyl)oxy]pyridine Tetraoxazole Macrocycle with a 1,3-Bis(aminomethyl)phenyl linker (23a). Using method D, **22** (45 mg, 0.071 mmol) was macrocyclized with 1,3-bis(aminomethyl)benzene (9 μ L, 0.071 mmol). The product, **23a** was obtained as a white solid; 18 mg (35%); mp 249–252 °C (dec). ¹H NMR δ 8.24 (s, 2H), 8.23 (s, 2H), 7.85 (dd, 2H, *J* = 3, 5), 7.72 (dd, 2H, *J* = 3, 5), 7.49 (m, 4H), 7.37 (m, 4H), 4.59 (d, 4H, *J* = 5), 4.27 (t, 2H, *J* = 6), 3.97 (t, 2H, *J* = 6), 2.30 (dt, 2H, *J* = 6, 12). ¹³C NMR δ 168.4, 166.7, 160.5, 159.7, 154.3, 146.8, 140.5, 138.8, 137.8, 137.5, 134.1, 132.1, 131.9, 129.9, 129.9, 129.5, 123.4, 109.4, 66.7, 43.9, 35.1, 28.0. HRMS (ESI) *m/z* calcd for C₃₈H₂₇N₈O₉ (M + H) 739.1896; found 739.1891.

4-[(3-Phthalimidopropyl)oxy]pyridine Tetraoxazole Macrocycle with a 1,3-Bis(aminomethyl)-5-bromophenyl Linker (23b). Using method D, **22** (22 mg, 0.034 mmol) was macrocyclized with **12** (10 mg, 0.034 mmol). The product, **23b** was obtained as a white solid; 3.3 mg (30%); mp 289–290 °C (dec). ¹H NMR (CDCl₃ + CD₃OD) δ 8.33 (s, 4H), 7.86 (dd, 2H, *J* = 3, 5), 7.75 (dd, 2H, *J* = 3, 5), 7.51 (m, 5H), 4.58 (s, 4H), 4.29 (t, 2H, *J* = 6), 3.98 (t, 2H, *J* = 7), 2.31 (dt, 2H, *J* = 6, 12). ¹³C NMR (CDCl₃ + CD₃OD) δ 168.6, 167.2, 160.9, 160.5, 154.3, 146.4, 141.6, 139.9, 139.3, 137.5, 134.4, 132.1, 131.9, 131.6, 128.7, 123.5, 122.8, 109.5, 66.9, 43.2, 35.1, 28.0. HRMS (ESI) *m/z* calcd for C₃₈H₂₆BrN₈O₉ (M + H) 817.1006; found 817.0986.

4-[(3-Phthalimidopropyl)oxy]pyridine Tetraoxazole Macrocycle with a 5-[2-(Benzylxycarbonylamino)ethyl-1,3-bis(aminomethyl)-5-bromophenyl Linker (23c). Using method D, **22** (21 mg, 0.033 mmol) was macrocyclized with **14b** (15 mg, 0.048 mmol). The product, **23c**, was obtained as a white solid; 11 mg (40%); mp 167–170 °C. ¹H NMR δ 8.24 (s, 2H), 8.23 (s, 2H), 7.85 (dd, 2H, *J* = 3, 5), 7.72 (dd, 2H, *J* = 3, 5), 7.56 (m, 2H), 7.47 (s, 2H), 7.27 (m, 5H), 7.17 (s, 3H), 5.04 (s, 2H), 4.95 (m, 1H), 4.56 (d, 4H, *J* = 4), 4.27 (t, 2H, *J* = 6), 3.97 (t, 2H, *J* = 6), 3.45 (m, 2H), 2.81 (m, 2H), 2.32 (dt, 2H, *J* = 6, 12). ¹³C NMR δ 168.4, 166.8, 160.5, 159.7, 156.3, 154.2, 146.7, 140.6, 138.8, 138.1, 137.4, 134.1, 132.1, 131.8, 130.0, 129.1, 128.4, 128.3, 128.2, 127.9, 125.3, 123.4, 109.4, 66.7, 43.8, 35.0, 28.0. HRMS (ESI) *m/z* calcd for C₄₈H₃₈N₉O₁₁ (M + H) 916.2691; found 916.2669.

4-[(3-Aminopropyl)oxy]pyridine Tetraoxazole Macrocycle with a 1,3-Bis(aminomethyl)phenyl Linker (23d). Hydrazine monohydrate (0.5 mL, 10.3 mmol) was added to a solution of **23a** (24 mg, 0.033 mmol) in EtOH (10 mL). The solution was heated at reflux for 3 h, cooled to room temperature, and concentrated under reduced pressure. The residue was dissolved in CH₂Cl₂, washed with 10% NaOH, and dried over Na₂SO₄. Evaporation of the solvent afforded **23d** as a white solid; 20 mg (100% yield); mp 237–239 °C (dec). ¹H NMR (CDCl₃ + CD₃OD) δ 8.32 (m, 4H), 7.57 (s, 3H), 7.36 (m, 3H), 4.63 (s, 4H), 4.27 (m, 2H), 2.94 (t, 2H, *J* = 6), 2.04 (dt, 2H, *J* = 6, 12). ¹³C NMR (CDCl₃ + CD₃OD) δ 167.4, 160.9, 160.3, 154.3, 146.4, 141.4, 139.4, 137.8, 137.5, 131.6, 130.2, 129.5, 129.2, 109.6, 66.7, 43.8, 38.4, 32.0. HRMS (ESI) *m/z* calcd for C₃₀H₂₅N₈O₇ (M + H) 609.1846; found 609.1825.

Cytotoxicity Assays. Cytotoxicity was determined using the MTT-microtiter plate tetrazolium assay (MTA). The human lymphoblast RPMI 8402 cell line was provided by Dr. Toshiwo Andoh (Aichi Cancer Center Research Institute, Nagoya, Japan).²³ The KB3-1 cell line and its multidrug-resistant variant KBV-1 were obtained from K. V. Chin (The Cancer Institute of New Jersey, New Brunswick, NJ).²⁴ The KBH5.0 cell line was derived from KB3-1 by stepwise selection against Hoechst 33342.²⁵ The cytotoxicity assay was performed using 96-well microtiter plates. Cells were grown in suspension at 37 °C in 5% CO₂ and maintained by regular passage in RPMI medium supplemented with 10% heat inactivated fetal bovine serum, L-glutamine (2 mM), penicillin (100 U/mL), and streptomycin (0.1 mg/mL). For determination of IC₅₀ values, cells were exposed continuously for four days to varying concentrations of drug and MTT assays were performed at the end of the fourth day. Each assay was performed with a control that did not contain any drug. All assays were performed at least twice in six replicate wells.

Temperature-Dependent Spectrophotometry. Temperature-dependent absorption experiments were conducted on an AIVIV model 14DS Spectrophotometer (Aviv Biomedical, Lakewood, NJ) equipped with a thermoelectrically controlled cell holder. Quartz cells with a path length of 1.0 cm were used for all the absorbance studies. Temperature-dependent absorption profiles were acquired at either 260 nm (for ST duplex DNA and poly(rA)·poly(rU) duplex RNA) or 295 nm (for hTel quadruplex DNA and AurA quadruplex RNA) with a 7 s averaging time. The temperature was raised in 0.5 °C increments, and the samples were allowed to equilibrate for 1 min at each temperature setting. In the quadruplex melting studies, the hTel and AurA concentrations were 5 μ M in strand. When present in these quadruplex studies, the drug concentrations were 20 μ M. In the duplex melting studies, the ST DNA concentrations were 30 μ M base pair, while the poly(rA)·poly(rU) concentrations were 15 μ M base pair. When present, the drug concentrations were 15 μ M in the ST DNA studies and 7.5 μ M in the poly(rA)·poly(rU) studies. The buffer for all the UV melting experiments contained 10 mM potassium phosphate (pH 7.5) and sufficient KCl (132 mM) to bring the total K⁺ concentration to 150 mM. Prior to their use in the UV melting experiments, all nucleic acid

solutions were preheated at 90 °C for 5 min and slowly cooled to room temperature over a period of 4 h.

Human Tumor Xenograft Assay. Bioassays were performed using female NCR/NU NU mice of approximately 9 weeks of age as obtained from Taconic Farms, Inc. (Germantown, NY). Mice were housed 3–4 per cage in laminar flow HEPA filtered microisolator caging (Allentown Caging Equipment Co., Allentown, NJ). Mice were fed Purina autoclavable breeder chow no. 5021 and given drinking water, purified by reverse-osmosis, ad libitum. Five days after arrival within the animal facility, the mice were inoculated on the right flank with 1.5×10^6 MDA-MB-435 tumor cells in 0.1 mL of RPMI 1640 Media by sc injection (25 gauge needle \times 5/8"). The MDA-MB-435 cells were grown in 75 cm² flasks using RPMI 1640 media and 10% fetal bovine serum. Tumors were of sufficient size at 19–20 days after inoculation. Tumor-bearing mice were evenly matched in each experimental group based on tumor volume. Mice were injected ip 3× weekly on alternate days. Negative controls consisted of seven mice that received 150 μ L of 10 mM citrate. The positive control group consisted of eight mice that received irinotecan (CPT-11, Camptosar) by ip injection at a dose of 20 mg/kg, 3× weekly, for all four weeks. Compound **19** was similarly administered to seven mice, 3× weekly, at doses of 0, 25, 32, and 42 mg/kg for weeks 1–4, respectively. Tumor volume was calculated by measuring the tumor with a microcaliper. The length (*l*) is the maximum two-dimensional distance of the tumor, and the width (*w*) is the maximum distance perpendicular to this length measured in mm. Tumor volume was calculated using the formula $(lw^2)/2$. Body weights and tumor volumes of individual mice were determined at a minimum of twice a week.

Acknowledgment. Financial support for this research was provided by Department of Defense grant W81XWH06-1-0514. The Bruker Avance III 400 NMR spectrometer used for this study was purchased with funds from NCRR grant no. 1S10RR23698-1A1. Mass spectrometry was provided by the Washington University Mass Spectrometry Resource with support from the NIH National Center for Research Resources (grant no. P41RR0954).

References

- (a) Han, H.; Hurley, L. H. G-Quadruplex DNA: a potential target for anti-cancer drug design. *TiPS* **2000**, *21*, 136–142. (b) Hurley, L. H.; Wheelhouse, R. T.; Sun, D.; Kerwin, S. M.; Salazar, M.; Fedoroff, O. Y.; Han, F. X.; Han, H.; Izbicka, E.; Von Hoff, D. D. G-Quadruplexes as targets for drug design. *Pharmacol. Ther.* **2000**, *85*, 141–158.
- (c) Neidle, S.; Read, M. A. G-Quadruplexes as therapeutic targets. *Biopolymers* **2001**, *56*, 195–208.
- (2) Shin-ya, K.; Wierzba, K.; Matsuo, K.-i.; Ohtani, T.; Yamada, Y.; Furihata, K.; Hayakawa, Y.; Seto, H. Telomestatin, a novel telomerase inhibitor from *Streptomyces anulatus*. *J. Am. Chem. Soc.* **2001**, *123*, 1262–1263.
- (3) Kim, M.-Y.; Vankayalapati, H.; Shin-ya, K.; Wierzba, K.; Hurley, L. H. Telomestatin, a potent telomerase inhibitor that interacts quite specifically with the human telomeric intramolecular G-quadruplex. *J. Am. Chem. Soc.* **2002**, *124*, 2098–2099.
- (4) Tahara, H.; Shin-ya, K.; Seimiya, H.; Yamada, H.; Tsuruo, T.; Ide, T. G-Quadruplex stabilization by telomestatin induces TRF2 protein dissociation from telomeres and anaphase bridge formation accompanied by loss of the 3' telomeric overhang in cancer cells. *Oncogene* **2006**, *25*, 1955–1966.
- (5) For representative examples see: (a) Sun, D.; Thompson, B.; Cathers, B. E.; Salazar, M.; Kerwin, S. M.; Trent, J. O.; Jenkins, T. C.; Neidle, S.; Hurley, L. H. Inhibition of human telomerase by a G-quadruplex-interactive compound. *J. Med. Chem.* **1997**, *40*, 2113–2116. (b) Wheelhouse, R. T.; Sun, D.; Han, H.; Han, F. X.; Hurley, L. H. Cationic porphyrins as telomerase inhibitors: The interaction of tetra-(N-methyl-4-pyridyl)porphine with quadruplex DNA. *J. Am. Chem. Soc.* **1998**, *120*, 3261–3262. (c) Fedoroff, O. Y.; Salazar, M.; Han, H.; Chemeris, V. V.; Kerwin, S. M.; Hurley, L. H. NMR-based model of a telomerase-inhibiting compound bound to G-quadruplex DNA. *Biochemistry* **1998**, *37*, 12367–12374. (d) Harrison, R. J.; Gowan, S. M.; Kelland, L. R.; Neidle, S. Human telomerase inhibition by substituted acridine derivatives. *Bioorg. Med. Chem. Lett.* **1999**, *9*, 2463–2468. (e) Koeppel, F.; Riou, J.-F.; Laoui, A.; Mailliet, P.; Arimondo, P. B.; Labit, D.; Petitgenet, O.; Hélène, C.; Mergny, J.-L. Ethidium derivatives bind to G-quartets, inhibit telomerase and act as fluorescent probes for quadruplexes. *Nucleic Acids Res.* **2001**, *29*, 1087–1096. (f) Duan, W.; Rangan, A.; Vankayalapati, H.; Kim, M.-Y.; Zeng, Q.; Sun, D.; Han, H.; Fedoroff, O. Y.; Nishioka, D.; Rha, S. Y.; Izbicka, E.; Von Hoff, D. D.; Hurley, L. H. Design and synthesis of fluoroquinophenoxazines that interact with human telomeric G-quadruplexes and their biological effects. *Mol. Cancer Ther.* **2001**, *1*, 103–120.
- (6) (a) Perry, P. J.; Jenkins, T. C. DNA tetraplex-binding drugs: structure-selective targeting is critical for antitumour telomerase inhibition. *Mini Rev. Med. Chem.* **2001**, *1*, 31–41. (b) Yu, H.; Wang, X.; Fu, M.; Ren, J.; Qu, X. Chiral metallo-supramolecular complexes selectively recognize human telomeric G-quadruplex DNA. *Nucleic Acids Res.* **2008**, *36*, 5695–5703. (c) Yu, H.; Zhao, C.; Chen, Y.; Fu, M.; Ren, M.; Qu, X. DNA loop sequence as the determinant for chiral supramolecular compound G-quadruplex selectivity. *J. Med. Chem.* **2010**, *53*, 492–498.
- (7) (a) Minhas, G. S.; Pilch, D. S.; Kerrigan, J. E.; LaVoie, E. J.; Rice, J. E. Synthesis and G-quadruplex stabilizing properties of a series of oxazole-containing macrocycles. *Bioorg. Med. Chem. Lett.* **2006**, *16*, 3891–3895. (b) Satyanarayana, M.; Rzuczek, S. G.; LaVoie, E. J.; Pilch, D. S.; Liu, A.; Liu, L. F.; Rice, J. E. Ring-closing metathesis for the synthesis of a highly G-quadruplex selective macrocyclic hexaoxazole having enhanced cytotoxic potency. *Bioorg. Med. Chem. Lett.* **2008**, *18*, 3802–3804. (c) Barbieri, C. M.; Srinivasan, A. R.; Rzuczek, S. G.; Rice, J. E.; LaVoie, E. J.; Pilch, D. S. Defining the mode, energetics and specificity with which a macrocyclic hexaoxazole binds to human telomeric G-quadruplex DNA. *Nucleic Acids Res.* **2007**, *35*, 3272–3286. (d) LaVoie, E. J.; Kim, Y. A.; Satyanarayana, M.; Rzuczek, S. G.; Pilch, D. S.; Tsai, Y.-C.; Qi, H.; Lin, C.-P.; Liu, A.; Liu, L. F.; Rice, J. E. Oxazole-containing macrocycles as selective G-quadruplex stabilizers. Molecular Targets and Cancer Therapeutics Proceedings, Boston, MA, November **2009**, p 275. (e) Satyanarayana, M.; Kim, Y.-A.; Rzuczek, S. G.; Pilch, D. S.; Liu, A. A.; Liu, L. F.; Rice, J. E.; LaVoie, E. J. Macrocyclic hexaoxazoles: Influence of aminoalkyl substituents on RNA and DNA G-quadruplex stabilization and cytotoxicity. *Bioorg. Med. Chem. Lett.* **2010**, in press.
- (8) (a) Binz, N.; Shalaby, T.; Rivera, P.; Shin-ya, K.; Grotzer, M. A. Telomerase inhibition, telomere shortening, cell growth suppression and induction of apoptosis by telomestatin in childhood neuroblastoma cells. *Eur. J. Cancer* **2005**, *41*, 2873–2881. (b) Liu, W.; Sun, D.; Hurley, L. H. Binding of G-quadruplex-interactive agents to distinct G-quadruplexes induces different biological effects in MiaPaCa cells. *Nucleosides, Nucleotides Nucleic Acids* **2005**, *24*, 1801–1815.
- (9) Tsai, Y.-C.; Qi, H.; Lin, C.-P.; Lin, R.-K.; Kerrigan, J. E.; Rzuczek, S. G.; LaVoie, E. J.; Rice, J. E.; Pilch, D. S.; Lyu, Y. L.; Liu, L. F. A G-Quadruplex stabilizer induces M phase cell cycle arrest. *J. Biol. Chem.* **2009**, *284*, 22535–22543.
- (10) (a) Rzuczek, S. G.; Pilch, D. S.; LaVoie, E. J.; Rice, J. E. Lysinyl macrocyclic hexaoxazoles: Synthesis and selective G-quadruplex stabilizing properties. *Bioorg. Med. Chem. Lett.* **2008**, *18*, 913–917. (b) Pilch, D. S.; Barbieri, C. M.; Rzuczek, S. G.; LaVoie, E. J.; Rice, J. E. Targeting human telomeric G-quadruplex DNA with oxazole-containing macrocyclic compounds. *Biochimie* **2008**, *90*, 1233–1249.
- (11) Philips, A. J.; Uto, Y.; Wipf, P.; Reno, M. J.; Williams, D. R. Synthesis of functionalized oxazolines and oxazoles with DAST and Deoxo-Fluor. *Org. Lett.* **2000**, *2*, 1165–1168.
- (12) Williams, D. R.; Lowder, P. D.; Gu, Y.-G.; Brooks, D. A. Studies of mild dehydrogenations in heterocyclic systems. *Tetrahedron Lett.* **1997**, *38*, 331–334.
- (13) Pryor, K. E.; Shipps, G. W., Jr.; Skyler, D. A.; Rebek, J., Jr. The activated core approach to combinatorial chemistry: a selection of new core molecules. *Tetrahedron* **1998**, *54*, 4107–4124.
- (14) Seebach, D.; Thaler, A.; Blaser, D.; Ko, S. Y. Transesterifications with 1,8-diazabicyclo[5.4.0]undec-7-ene/lithium bromide (DBU/LiBr)—also applicable to cleavage of peptides from resins in Merrifield syntheses. *Helv. Chim. Acta* **1991**, *74*, 1102–1118.
- (15) Shibatomi, K. Preparation of optically active 2,6-bis(aminomethyl)-pyridines and asymmetric reactions with their metal complex catalysts. *Jpn. Kokai Tokkyo Koho* JP 2008024596 A 20080207, 2008.
- (16) Fritz, H.; Hug, P.; Lawesson, S. O.; Logemann, E.; Pedersen, B. S.; Sauter, H.; Scheibley, S.; Winkler, T. Studies on organophosphorus compounds. XXVI. Synthesis and carbon-13 NMR spectra of *N,N*-dialkyl thioamides. *Bull. Soc. Chim. Belg.* **1978**, *87*, 525–534.
- (17) Manabe, K. Synthesis of novel chiral quaternary phosphonium salts with a multiple hydrogen-bonding site, and their application to asymmetric phase-transfer alkylation. *Tetrahedron* **1998**, *54*, 14465–14476.

(18) (a) Molander, G. A.; Vargas, F. β -Aminoethyltrifluoroborates: efficient aminoethylations via Suzuki–Miyaura cross-coupling. *Org. Lett.* **2007**, *9*, 203–206. (b) Molander, G. A.; Jean-Gérard, L. Scope of the Suzuki–Miyaura aminoethylation reaction using organotrifluoroborates. *J. Org. Chem.* **2007**, *72*, 8422–8426.

(19) Luu, K. N.; Phan, A. T.; Kuryavyi, V.; Lacroix, L.; Patel, D. J. Structure of the human telomere in K⁺ solution: An intramolecular (3 + 1) G-quadruplex scaffold. *J. Am. Chem. Soc.* **2006**, *128*, 9963–9970.

(20) (a) Crothers, D. M. Statistical thermodynamics of nucleic acid melting transitions with coupled binding equilibria. *Biopolymers* **1971**, *10*, 2147–2160. (b) McGhee, J. D. Theoretical calculations of the helix–coil transition of DNA in the presence of large, cooperatively binding ligands. *Biopolymers* **1976**, *15*, 1345–1375.

(21) Tauchi, T.; Shin-ya, K.; Sashida, G.; Sumi, M.; Okabe, S.; Ohyashiki, J. H.; Ohyashiki, K. Telomerase inhibition with a novel G-quadruplex-interacting agent, telomestatin: in vitro and in vivo studies in acute leukemia. *Oncogene* **2006**, *25*, 5719–5725.

(22) Plum, G. E. Optical methods. In *Current Protocols in Nucleic Acid Chemistry*, Vol. 1; Beaucage, S. L., Bergstrom, D. E., Glick, G. D., Jones, R. A., Eds.; John Wiley & Sons, New York, 2000; pp 7.3.1–7.3.17.

(23) Andoh, T.; Ishii, K.; Suzuki, Y.; Ikegami, Y.; Kusunoki, Y.; Takemoto, Y.; Okada, K. Characterization of a mammalian mutant with a camptothecin-resistant DNA topoisomerase I. *Proc. Natl. Acad. Sci. U.S.A.* **1987**, *84*, 5565–5569.

(24) Gervasoni, J. E., Jr.; Fields, S. Z.; Krishna, S.; Baker, M. A.; Rosado, M.; Thuraisamy, K.; Hindenbug, A. A.; Taub, R. N. Subcellular distribution of daunorubicin in p-glycoprotein-positive and negative drug-resistant cell lines using laser-assisted confocal microscopy. *Cancer Res.* **1991**, *51*, 4955–4963.

(25) Li, T.-K.; Houghton, P. J.; Desai, S. D.; Darou, P.; Liu, A. A.; Hars, E. S.; Ruchelman, A. L.; LaVoie, E. J.; Liu, L. F. Characterization of ARC-111 as a novel topoisomerase I-targeting anticancer drug. *Cancer Res.* **2003**, *63*, 8400–8407.